NONPERTURBATIVE FLOW EQUATIONS, LOW–ENERGY QCD AND THE CHIRAL PHASE TRANSITION

D.–U. Jungnickel and C. Wetterich*

Institut für Theoretische Physik,
Universität Heidelberg, Philosophenweg 16,
69120 Heidelberg, Germany

EFFECTIVE AVERAGE ACTION

Quantum chromodynamics (QCD) describes qualitatively different physics at different length scales. At short distances the relevant degrees of freedom are quarks and gluons which can be treated perturbatively. At long distances we observe hadrons, and an essential part of the dynamics can be encoded in the masses and interactions of mesons. Any attempt to deal with this situation analytically and to predict the meson properties from the short distance physics (as functions of the strong gauge coupling α_s and the current quark masses m_q) has to bridge the gap between two qualitatively different effective descriptions. Two basic problems have to be mastered for an extrapolation from short distance QCD to mesonic length scales:

- The effective couplings change with scale. This does not only concern the running gauge coupling, but also the coefficients of non–renormalizable operators as, for example, four quark operators. Typically, these non–renormalizable terms become important in the momentum range where α_s is strong and deviate substantially from their perturbative values. Consider the four–point function which results after integrating out the gluons. For heavy quarks it contains the information about the shape of the heavy quark potential whereas for light quarks the complicated spectrum of light mesons and chiral symmetry breaking are encoded in it. At distance scales around 1 fm one expects that the effective action resembles very little the form of the classical QCD action which is relevant at short distances.

- Not only the couplings, but even the relevant variables or degrees of freedom are different for long distance and short distance QCD. It seems forbiddingly difficult to describe the low–energy scattering of two mesons in a language of quarks and gluons only. An appropriate analytical field theoretical method should be capable of introducing field variables for composite objects such as mesons.

A conceptually very appealing idea for our task is the block–spin action[1, 2]. It realizes

*Lectures presented by Christof Wetterich that physics with a given characteristic length scale l is conveniently described by a functional integral with an ultraviolet (UV) cutoff Λ for the momenta. Here Λ should be larger than l^{-1} but not necessarily by a large factor. The Wilsonian effective action S_Λ^{W} replaces then the classical action in the functional integral. It is obtained by integrating out the fluctuations with momenta $q^2 \gtrsim \Lambda^2$. An exact renormalization group equation[2, 3, 4, 5, 6] describes how S_Λ^{W} changes with the UV cutoff Λ.

We will use here the somewhat different but related concept of the effective average action[7] Γ_k which, in the language of statistical physics, is a coarse grained free energy with coarse graining scale k. The effective average action is based on the quantum field theoretical concept of the effective action[8] Γ which is obtained by integrating out all quantum fluctuations. The effective action contains all information about masses, couplings, form factors and so on, since it is the generating functional of the $1PI$ Green functions. The field equations derived from Γ are exact including all quantum effects. For a field theoretical description of thermal equilibrium this concept is easily generalized to a temperature dependent effective action which includes now also the thermal fluctuations. In statistical physics Γ describes the free energy as a functional of some convenient (space dependent) order parameter, for instance the magnetization. In particular, the behavior of Γ for a constant order parameter (the effective potential) specifies the equation of state. The effective average action Γ_k is a simple generalization of the effective action, with the distinction that only quantum fluctuations with momenta $q^2 \gtrsim k^2$ are included. This can be achieved by introducing an explicit infrared cutoff $\sim k$ in the functional integral defining the partition function (or the generating functional for the n–point functions). Typically, this IR–cutoff is quadratic in the fields and modifies the inverse propagator, for example by adding a mass–like term $\sim k^2$. The effective average action can then be defined in complete analogy to the effective action (via a Legendre transformation of the logarithm of the partition function). The mass–like term in the propagator suppresses the contributions from the small momentum modes with $q^2 \lesssim k^2$ and Γ_k accounts effectively only for the fluctuations with $q^2 \gtrsim k^2$.

Following the behavior of Γ_k for different k is like looking at the world through a microscope with variable resolution: For large k one has a very precise resolution $\sim k^{-1}$ but one also studies effectively only a small volume $\sim k^d$. Taking in QCD the coarse graining scale k much larger than the confinement scale guarantees that the complicated nonperturbative physics does not play a role yet. In this case, Γ_k will look similar to the classical action, typically with a running gauge coupling evaluated at the scale k. (This does not hold for Green functions with much larger momenta $p^2 \gg k^2$ where the relevant IR cutoff is p, and the effective coupling is $\alpha_s(p)$.) For lower k the resolution is smeared out and the detailed information of the short distance physics can be lost. (Again, this does not concern Green functions at high momenta.) On the other hand, the "observable volume" is increased and long distance aspects such as collective phenomena become visible. In a theory with a physical UV cutoff Λ we may associate Γ_Λ with the classical action S since no fluctuations are effectively included. By definition, the effective average action equals the effective action for $k = 0$, $\Gamma_0 = \Gamma$, since the infrared cutoff is absent. Thus Γ_k interpolates between the classical action S and the effective action Γ as k is lowered from Λ to zero. The ability to follow the evolution $k \to 0$ is equivalent to the ability to solve the quantum field theory.

For a formal description we will consider in the first two sections a model with real scalar fields χ^a (the index a labeling internal degrees of freedom) in d Euclidean dimensions with classical action $S[\chi]$. We define the generating functional for the connected Green functions by

$$W_k[J] = \ln \int \mathcal{D}\chi \exp\left\{-S_k[\chi] + \int d^d x J_a(x)\chi^a(x)\right\} \tag{1}$$

where we have added to the classical action an IR cutoff $\Delta_k S$

$$S_k[\chi] = S[\chi] + \Delta S_k[\chi] \tag{2}$$

which is quadratic in the fields and conveniently formulated in momentum space

$$\Delta S_k[\chi] = \frac{1}{2}\int \frac{d^d q}{(2\pi)^d} R_k(q^2)\chi_a(-q)\chi^a(q) \ . \tag{3}$$

Here J_a are the usual scalar sources introduced to define generating functionals and $R_k(q^2)$ denotes an appropriately chosen (see below) IR cutoff function. We require that $R_k(q^2)$ vanishes rapidly for $q^2 \gg k^2$ whereas for $q^2 \ll k^2$ it behaves as $R_k(q^2) \simeq k^2$. This means that all Fourier components of χ^a with momenta smaller than the IR cutoff k acquire an effective mass $m_{\mathrm{eff}} \simeq k$ and therefore decouple while the high momentum components of χ^a should not be affected by R_k. The classical fields

$$\Phi^a \equiv \langle \chi^a \rangle = \frac{\delta W_k[J]}{\delta J_a} \tag{4}$$

now depend on k. In terms of W_k the effective average action is defined via a Legendre transformation

$$\Gamma_k[\Phi] = -W_k[J] + \int d^d x J_a(x)\Phi^a(x) - \Delta S_k[\Phi] \ . \tag{5}$$

In order to define a reasonable coarse grained free energy we have subtracted in Eq.(5) the infrared cutoff piece. This guarantees that the only difference between Γ_k and Γ is the effective IR cutoff in the fluctuations. Furthermore, this has the consequence that Γ_k does not need to be convex whereas a pure Legendre transform is always convex by definition. (The coarse grained free energy becomes convex[9] only for $k \to 0$.) This is very important for the description of phase transitions, in particular first order ones. One notes

$$\begin{aligned} \lim_{k\to 0} R_k(q^2) = 0 \quad &\Rightarrow \quad \lim_{k\to 0} \Gamma_k[\Phi] = \Gamma[\Phi] \\ \lim_{k\to \Lambda} R_k(q^2) = \infty \quad &\Rightarrow \quad \lim_{k\to \Lambda} \Gamma_k[\Phi] = S[\Phi] \end{aligned} \tag{6}$$

for a convenient choice of R_k like

$$R_k(q^2) = Z_{\Phi,k} q^2 \frac{1 + e^{-q^2/k^2} - e^{-q^2/\Lambda^2}}{e^{-q^2/\Lambda^2} - e^{-q^2/k^2}} \ . \tag{7}$$

Here $Z_{\Phi,k}$ denotes the wave function renormalization to be specified below and we will often use for R_k the limit $\Lambda \to \infty$

$$R_k(q^2) = \frac{Z_{\Phi,k} q^2}{e^{q^2/k^2} - 1} \ . \tag{8}$$

We note that the property $\Gamma_\Lambda = S$ is not essential since the short distance laws may be parameterized by Γ_Λ as well as by S. In addition, for momentum scales much smaller than Λ universality implies that the precise form of Γ_Λ is irrelevant, up to the values of a few relevant renormalized couplings.

A few properties of the effective average action are worth mentioning:

1. All symmetries of the model which are respected by the IR cutoff $\Delta_k S$ are automatically symmetries of Γ_k. In particular, this concerns translation and rotation invariance and one is not plagued by many of the problems encountered by a formulation of the block–spin action on a lattice.

2. In consequence, Γ_k can be expanded in terms of invariants with respect to these symmetries with couplings depending on k. For the example of a scalar theory one may use a derivative expansion ($\rho = \Phi^a\Phi_a/2$)

$$\Gamma_k = \int d^dx \left\{ U_k(\rho) + \frac{1}{2} Z_{\Phi,k}(\rho)\partial^\mu\Phi_a\partial_\mu\Phi^a + \ldots \right\} \tag{9}$$

and expand further in powers of ρ

$$\begin{aligned} U_k(\rho) &= \frac{1}{2}\overline{\lambda}_k\left(\rho-\rho_0(k)\right)^2 + \frac{1}{6}\overline{\gamma}_k\left(\rho-\rho_0(k)\right)^3 + \ldots \\ Z_{\Phi,k}(\rho) &= Z_{\Phi,k}(\rho_0) + Z'_{\Phi,k}(\rho_0)\left(\rho-\rho_0\right) + \ldots \end{aligned} \tag{10}$$

where ρ_0 denotes the (k–dependent) minimum of the effective average potential $U_k(\rho)$. We see that Γ_k describes infinitely many running couplings. ($Z_{\Phi,k}$ in Eq.(7) can be identified with $Z_{\Phi,k}(\rho_0)$.)

3. There is no problem incorporating chiral fermions since a chirally invariant cutoff R_k can be formulated[10, 11].

4. Gauge theories can be formulated along similar lines[12, 13, 14, 15, 16, 17] even though $\Delta_k S$ may not be gauge invariant. In this case the usual Ward identities receive corrections for which one can derive closed expressions[15]. These corrections vanish for $k \to 0$.

5. The high momentum modes are very effectively integrated out because of the exponential decay of R_k for $q^2 \gg k^2$. Nevertheless, it is sometimes technically easier to use a cutoff without this fast decay property (e.g. $R_k \sim k^2$ or $R_k \sim k^4/q^2$). In the latter case one has to be careful with possible remnants of an incomplete integration of the short distance modes. Also our cutoff does not introduce any non–analytical behavior as would be the case for a sharp cutoff[7].

6. Despite a similar spirit and many analogies there remains also a conceptual difference to the Wilsonian effective action S_Λ^{W}. The Wilsonian effective action describes a set of different actions (parameterized by Λ) for one and the same theory — the n–point functions are independent of Λ and have to be computed from S_Λ^{W} by further functional integration. In contrast, Γ_k describes the effective action for different theories — for any value of k the effective average action is related to the generating functional of a theory with a different action $S_k = S + \Delta_k S$. The n–point functions depend on k. The Wilsonian effective action does not generate the $1PI$ Green functions[19].

7. Because of the incorporation of an infrared cutoff, Γ_k is closely related to an effective action for averages of fields[7], where the average is taken over a volume $\sim k^d$.

EXACT RENORMALIZATION GROUP EQUATION

The dependence of Γ_k on the coarse graining scale k is governed by an exact renormalization group equation (ERGE)[20]

$$\partial_t\Gamma_k[\Phi] = \frac{1}{2}\,\mathrm{Tr}\left\{\left[\Gamma_k^{(2)}[\Phi] + R_k\right]^{-1}\partial_t R_k\right\}\ . \tag{11}$$

Here $t = \ln(k/\Lambda)$ with some arbitrary momentum scale Λ, and the trace includes a momentum integration as well as a summation over internal indices, $\mathrm{Tr} = \int \frac{d^dq}{(2\pi)^d} \sum_a$. The second functional derivative $\Gamma_k^{(2)}$ denotes the *exact* inverse propagator

$$\left[\Gamma_k^{(2)}\right]_{ab}(q, q') = \frac{\delta^2 \Gamma_k}{\delta \Phi^a(-q) \delta \Phi^b(q')} \ . \tag{12}$$

The flow equation Eq.(11) can be derived from Eq.(5) in a straightforward way using

$$\begin{aligned} \partial_t \left. \Gamma_k \right|_\Phi &= - \partial_t \left. W_k \right|_J - \partial_t \Delta_k S[\Phi] \\ &= \frac{1}{2} \mathrm{Tr} \left\{ \partial_t R_k \left(\langle \Phi \Phi \rangle - \langle \Phi \rangle \langle \Phi \rangle \right) \right\} \\ &= \frac{1}{2} \mathrm{Tr} \left\{ \partial_t R_k W_k^{(2)} \right\} \end{aligned} \tag{13}$$

and

$$\begin{aligned} W_{k,ab}^{(2)}(q, q') &= \frac{\delta^2 W_k}{\delta J^a(-q) \delta J^b(q')} \\ \frac{\delta^2 W_k}{\delta J_a(-q) \delta J_b(q')} \frac{\delta^2 \left(\Gamma_k + \Delta_k S \right)}{\delta \Phi_b(-q') \delta \Phi_c(q'')} &= \delta_{ac} \delta_{qq''} \ . \end{aligned} \tag{14}$$

It has the form of a renormalization group improved one–loop expression[7]. Indeed, the one–loop formula for Γ_k reads

$$\Gamma_k[\Phi] = S[\Phi] + \frac{1}{2} \mathrm{Tr} \ln \left(S^{(2)}[\Phi] + R_k \right) \tag{15}$$

with $S^{(2)}$ the second functional derivative of the *classical* action, similar to Eq.(12). (Remember that $S^{(2)}$ is the field dependent classical inverse propagator. Its first and second derivative with respect to the fields describe the classical three– and four–point vertices, respectively.) Taking a t–derivative of Eq.(15) gives a one–loop flow equation very similar to Eq.(11) with $\Gamma_k^{(2)}$ replaced by $S^{(2)}$. It may seem surprising, but it is nevertheless true, that the renormalization group improvement $S^{(2)} \to \Gamma_k^{(2)}$ promotes the one–loop flow equation to an exact nonperturbative flow equation which includes the effects from all loops as well as all contributions which are non–analytical in the couplings like instantons, etc.! For practical computations it is actually often quite convenient to write the flow equation Eq.(11) as a formal derivative of a renormalization group improved one–loop expression

$$\partial_t \Gamma_k = \frac{1}{2} \mathrm{Tr} \, \tilde{\partial}_t \ln \left(\Gamma_k^{(2)} + R_k \right) \tag{16}$$

with $\tilde{\partial}_t$ acting only on R_k and not on $\Gamma_k^{(2)}$, i.e. $\tilde{\partial}_t = (\partial R_k / \partial t)(\partial / \partial R_k)$. Flow equations for n–point functions follow from appropriate functional derivatives of Eq.(11) or Eq.(16) with respect to the fields. For their derivation it is sufficient to evaluate the corresponding one–loop expressions (with the vertices and propagators derived from Γ_k) and then to take a formal $\tilde{\partial}_t$–derivative. (If the one–loop expression is finite or properly regularized the $\tilde{\partial}_t$–derivative can be taken after the evaluation of the trace.) This permits the use of (one–loop) Feynman diagrams and standard perturbative techniques in many circumstances. Most importantly, it establishes a very direct connection between the solution of flow–equations and perturbation theory. If one uses on the right hand side of Eq.(11) a truncation for which the propagator and vertices appearing in

$\Gamma_k^{(2)}$ are replaced by the ones derived from the classical action, but with running k–dependent couplings, and then expands the result to lowest non–trivial order in the coupling constants one recovers standard renormalization group improved one–loop perturbation theory. The formal solution of the flow equation can also be employed for the development of a systematically resummed perturbation theory[21].

For a choice of the cutoff function similar to Eq.(8) the momentum integral contained in the trace on the right hand side of the flow equation is both infrared and ultraviolet finite. Infrared finiteness arises through the presence of the infrared regulator $\sim R_k$. We note that all eigenvalues of the matrix $\Gamma_k^{(2)} + R_k$ must be positive semi–definite. The proof follows from the observation that the functional $\Gamma_k + \Delta_k S$ is convex since it is obtained from W_k by a Legendre transform. On the other hand, ultraviolet finiteness is related to the fast decay of $\partial_t R_k$ for $q^2 \gg k^2$. This expresses the fact that only a narrow range of fluctuations with $q^2 \simeq k^2$ contributes effectively if the infrared cutoff k is lowered by a small amount. If for some other choice of R_k the right hand side of the flow equation would not remain UV finite this would indicate that the high momentum modes have not yet been integrated out completely in the computation of Γ_k. Since the flow equation is manifestly finite this can be used to define a regularization scheme. The "ERGE–scheme" is specified by the flow equation, the choice of R_k and the "initial condition" Γ_Λ. This is particularly important for gauge theories where other regularizations in four dimensions and in the presence of chiral fermions are difficult to construct. For gauge theories Γ_Λ has to obey appropriately modified Ward identities. In the context of perturbation theory a first proposal how to regularize gauge theories by use of flow equations can be found in[13, 14]. We note that in contrast to previous versions of exact renormalization group equations there is no need in the present formulation to construct an ultraviolet momentum cutoff — a task known to be very difficult in non–Abelian gauge theories.

Despite the conceptual differences between the Wilsonian effective action S_Λ^{W} and the effective average action Γ_k the exact flow equations describing the Λ–dependence of S_Λ^{W} and the k–dependence of Γ_k are simply related. Polchinski's continuum version of the Wilsonian flow equation[5] can be transformed into Eq.(11) by means of a Legendre transform and a suitable variable redefinition[22].

Even though intuitively simple, the replacement of the (RG–improved) classical propagator by the full propagator turns the solution of the flow equation Eq.(11) into a difficult mathematical problem: The evolution equation is a functional differential equation. Once Γ_k is expanded in terms of invariants (e.g. Eqs.(9), (10)) this is equivalent to a coupled system of non–linear partial differential equations for infinitely many couplings. General methods for the solution of functional differential equations are not developed very far. They are mainly restricted to iterative procedures that can be applied once some small expansion parameter is identified. This covers usual perturbation theory in the case of a small coupling, the $1/N$–expansion or expansions in the dimensionality $4-d$ or $2-d$. It may also be extended to less familiar expansions like a derivative expansion which is related in critical three dimensional scalar theories to a small anomalous dimension. In the absence of a clearly identified small parameter one nevertheless needs to truncate the most general form of Γ_k in order to reduce the infinite system of coupled differential equations to a (numerically) manageable size. This truncation is crucial. It is at this level that approximations have to be made and, as for all nonperturbative analytical methods, they are often not easy to control. The challenge for nonperturbative systems like low momentum QCD is to find flow equations which (a) incorporate all the relevant dynamics such that neglected effects make only small changes, and (b) remain of manageable size. The difficulty with the first task is a reliable estimate of the error. For the second task the main limitation is a practical restriction for numerical solutions of differential equations to functions depending only on a small number of variables. The existence of an exact functional differential flow equation is a very useful starting point and guide for this task. At this point the precise form of the exact flow equation is quite important. Furthermore, it can be used for systematic expansions through enlargement of the truncation and for an error estimate in this way. Nevertheless, this is not all. Usually, physical insight into a model is necessary to device a useful nonperturbative truncation!

So far, two complementary approaches to nonperturbative truncations have been explored: an expansion of the effective Lagrangian in powers of derivatives ($\rho \equiv \frac{1}{2}\Phi_a \Phi^a$)

$$\Gamma_k[\Phi] = \int d^d x \left\{ U_k(\rho) + \frac{1}{2} Z_{\Phi,k}(\Phi) \partial_\mu \Phi^a \partial^\mu \Phi_a + \frac{1}{4} Y_{\Phi,k}(\rho) \partial_\mu \rho \partial^\mu \rho + \mathcal{O}(\partial^4) \right\} \tag{17}$$

or one in powers of the fields

$$\Gamma_k[\Phi] = \sum_{n=0}^{\infty} \frac{1}{n!} \int \left(\prod_{j=0}^{n} d^d x_j \left[\Phi(x_j) - \Phi_0 \right] \right) \Gamma_k^{(n)}(x_1, \ldots, x_n) \, . \tag{18}$$

If one chooses Φ_0 as the k–dependent VEV of Φ, the series Eq.(18) starts effectively at $n = 2$. The flow equations for the $1PI$ n–point functions $\Gamma_k^{(n)}$ are obtained by functional differentiation of Eq.(11). Such flow equations have been discussed earlier from a somewhat different viewpoint[4]. They can also be interpreted as a differential form of Schwinger–Dyson equations[23].

The formation of mesonic bound states, which typically appear as poles in the (Minkowskian) four–quark Green function, is most efficiently described by expansions like Eq.(18). This is also the form needed to compute the nonperturbative momentum dependence of the gluon propagator and the heavy quark potential[16, 17, 18]. On the other hand, a parameterization of Γ_k as in Eq.(17) seems particularly suited for the study of phase transitions. The evolution equation for the average potential U_k follows by evaluating Eq.(17) for constant Φ. In the limit where the Φ–dependence of $Z_{\Phi,k}$ is neglected and $Y_{\Phi,k} = 0$ one finds[7] for the $O(N)$–symmetric scalar model

$$\partial_t U_k(\rho) = \frac{1}{2} \int \frac{d^d q}{(2\pi)^d} \frac{\partial R_k}{\partial t} \left(\frac{N-1}{Z_{\Phi,k} q^2 + R_k + U_k'} + \frac{1}{Z_{\Phi,k} q^2 + R_k(q) + U_k' + 2\rho U_k''} \right) \tag{19}$$

with $U_k' \equiv \frac{\partial U_k}{\partial \rho}$, etc. One observes the appearance of ρ–dependent mass terms in the effective propagators of the right hand side of Eq.(19). Once $\eta_\Phi \equiv -\partial_t \ln Z_{\Phi,k}$ is determined[7] in terms of the couplings parameterizing U_k this is a partial differential equation. for a function U_k depending on two variables k and ρ which can be solved numerically[24, 25, 26, 27]. (The Wilson–Fisher fixed point relevant for a second order phase transition ($d = 3$) corresponds to a scaling solution[28, 29] where $\partial_t U_k = 0$.) A suitable truncation of a flow equation of the type Eq.(17) will play a central role in the description of chiral symmetry breaking below.

It should be mentioned at this point that the weakest point in the ERGE approach seems to be a reliable estimate of the truncation error in a nonperturbative context. This problem is common to all known analytical approaches to nonperturbative phenomena and appears often even within systematic (perturbative) expansions. One may hope that the existence of an exact flow equation could also be of some help for error estimates. An obvious possibility to test a given truncation is its enlargement to include more variables — for example, going one step higher in a derivative expansion. This is similar to computing higher orders in perturbation theory and limited by practical considerations. As an alternative, one may employ different truncations of comparable size — for instance, by using different definitions of retained couplings. A comparison of the results can give a reasonable picture of the uncertainty if the used set of truncations is wide enough. In this context we should also note the dependence of the results on the choice of the cutoff function $R_k(q)$. Of course, for $k \to 0$ the physics should not depend on a particular choice of R_k and, in fact, it does not for full solutions of Eq.(11). Different choices of R_k just correspond to different trajectories in the space of effective average actions along which the unique IR limit $\Gamma[\Phi]$ is reached. Once approximations are used to solve the ERGE Eq.(11), however, not only the trajectory but also its end point will depend on the precise definition of the function R_k. This is very similar to the renormalization scheme dependence usually encountered in perturbative computations of Green functions. One may use this scheme dependence as a tool to study the robustness of a given approximation scheme.

Before applying a new nonperturbative method to a complicated theory like QCD it should be tested for simpler models. A good criterion for the capability of the ERGE to deal with nonperturbative phenomena concerns the critical behavior in three dimensional scalar theories. In a first step the well known results of other methods for the critical exponents have been reproduced within a few percent accuracy[28]. The ability of the method to produce new results has been demonstrated by the computation of the critical equation of state for Ising and Heisenberg models[25] which has been verified by lattice simulations[30]. This has been extended to first order transitions in matrix models[27] or for the Abelian Higgs model relevant for superconductors[31, 26]. Analytical investigations of the high temperature phase transitions in $d = 4$ scalar theories ($O(N)$–models) have correctly described the second order nature of the transition[32], in contrast to earlier attempts within high temperature perturbation theory.

For an extension of the flow equations to Abelian and non–Abelian gauge theories we refer the reader to[12, 13, 14, 15, 16, 17, 18]. The other necessary piece for a description of low–energy QCD, namely the transition from fundamental (quark and gluon) degrees of freedom to composite (meson) fields within the framework of the ERGE can be found in[33]. We will describe the most important aspects of this formalism for mesons below.

CHIRAL SYMMETRY BREAKING IN QCD

The strong interaction dynamics of quarks and gluons at short distances or high energies is successfully described by quantum chromodynamics (QCD). One of its most striking features is asymptotic freedom[34] which makes perturbative calculations reliable in the high energy regime. On the other hand, at scales around a few hundred MeV confinement sets in. As a consequence, the low–energy degrees of freedom in strong interaction physics are mesons, baryons and glueballs rather than quarks and gluons. When constructing effective models for these IR degrees of freedom one usually relies on the symmetries of QCD as a guiding principle, since a direct derivation of such models from QCD is still missing. The most important symmetry of QCD, its local color $SU(3)$ invariance, is of not much help here, since the IR spectrum appears to be color neutral. When dealing with bound states involving heavy quarks the so called "heavy quark symmetry" may be invoked to obtain approximate symmetry relations between IR observables[35]. We will rather focus here on the light scalar and pseudoscalar meson spectrum and therefore consider QCD with only the light quark flavors u, d and s. To a good approximation the masses of these three flavors can be considered as small in comparison with other typical strong interaction scales. One may therefore consider the chiral limit of QCD (vanishing current quark masses) in which the classical QCD Lagrangian does not couple left– and right–handed quarks. It therefore exhibits a global chiral invariance under $U_L(N) \times U_R(N) = SU_L(N) \times SU_R(N) \times U_V(1) \times U_A(1)$ where N denotes the number of massless quarks ($N = 2$ or 3) which transform as

$$\begin{aligned} \psi_R \equiv \frac{1-\gamma_5}{2}\psi \longrightarrow \mathcal{U}_R\psi_R \; ; \quad \mathcal{U}_R \in U_R(N) \\ \psi_L \equiv \frac{1+\gamma_5}{2}\psi \longrightarrow \mathcal{U}_L\psi_L \; ; \quad \mathcal{U}_L \in U_L(N) \; . \end{aligned} \tag{20}$$

Even for vanishing quark masses only the diagonal $SU_V(N)$ vector–like subgroup can be observed in the hadron spectrum ("eightfold way"). The symmetry $SU_L(N) \times SU_R(N)$ must therefore be spontaneously broken to $SU_V(N)$

$$SU_L(N) \times SU_R(N) \longrightarrow SU_{L+R}(N) \equiv SU_V(N) \; . \tag{21}$$

Chiral symmetry breaking is one of the most prominent features of strong interaction dynamics and phenomenologically well established[36], though a rigorous derivation of this phenomenon starting from first principles is still missing. In particular, the chiral symmetry breaking Eq.(21) predicts for $N = 3$ the existence of eight light parity–odd (pseudo–)Goldstone bosons: π^0, $\pi^\pm$, K^0, $\overline{K}^0$, $K^\pm$ and η. Their comparably small masses are a consequence of the explicit chiral symmetry breaking due to small but non–vanishing current quark masses. The axial Abelian subgroup $U_A(1) = U_{L-R}(1)$ is broken in the quantum theory by an anomaly of the axial–vector current. This breaking proceeds without the occurrence of a Goldstone boson[37]. Finally, the $U_V(1) = U_{L+R}(1)$ subgroup corresponds to baryon number conservation.

The light pseudoscalar and scalar mesons are thought of as color neutral quark–antiquark bound states $\Phi^{ab} \sim \overline{\psi}_L^b \psi_R^a$, $a, b = 1, \ldots, N$, which therefore transform under chiral rotations Eq.(20) as

$$\Phi \longrightarrow \mathcal{U}_R \Phi \mathcal{U}_L^\dagger \; . \tag{22}$$

Hence, the chiral symmetry breaking pattern Eq.(21) is realized if the meson potential develops a VEV

$$\left\langle \Phi^{ab} \right\rangle = \overline{\sigma}_0 \delta^{ab} \; ; \quad \overline{\sigma}_0 \neq 0 \; . \tag{23}$$

One of the most crucial and yet unsolved problems of strong interaction dynamics is to derive an effective field theory for the mesonic degrees of freedom directly from QCD which exhibits this behavior.

A SEMI–QUANTITATIVE PICTURE

Before turning to a quantitative description of chiral symmetry breaking using flow equations it is perhaps helpful to give a brief overview of the relevant scales which appear in relation to this phenomenon and the physical degrees of freedom associated to them. Some of this will be explained in more detail in the remainder of these lectures whereas other parts are rather well established features of strong interaction physics.

At scales above approximately 1.5 GeV, the relevant degrees of freedom of strong interactions are quarks and gluons and their dynamics appears to be well described by perturbative QCD. At somewhat lower energies this changes dramatically. Quark and gluon bound states form and confinement sets in. Concentrating on the physics of scalar and pseudoscalar mesons† there are three important momentum scales which appear to be rather well separated:

†One may assume that all other bound states are integrated out. We will comment on this issue below.

- The compositeness scale k_Φ at which mesonic $\overline{\psi}\psi$ bound states form because of the increasing strength of the strong interaction. It will turn out to be somewhere in the range $(600 - 700)\,\mathrm{MeV}$.

- The chiral symmetry breaking scale $k_{\chi SB}$ at which the chiral condensate $\left\langle \overline{\psi}^b \psi^a \right\rangle$ or $\left\langle \Phi^{ab} \right\rangle$ assumes a non–vanishing value, therefore breaking chiral symmetry according to Eq.(21). This scale is found to be around $(400 - 500)\,\mathrm{MeV}$. For k below $k_{\chi SB}$ the quarks acquire constituent masses $M_q \simeq 350\,\mathrm{MeV}$ due to their Yukawa coupling to the chiral condensate Eq.(23).

- The confinement scale $\Lambda_{\mathrm{QCD}} \simeq 200\,\mathrm{MeV}$ which corresponds to the Landau pole in the perturbative evolution of the strong coupling constant α_s. In our context, this is the scale where possible deviations of the effective quark propagator from its classical form and multi–quark interactions not included in the meson physics may become very important.

For scales k in the range $k_{\chi SB} \lesssim k \lesssim k_\Phi$ the most relevant degrees of freedom are mesons and quarks. Typically, the dynamics in this range is dominated by the strong Yukawa coupling h between quarks and mesons: $h^2/(4\pi) \gg \alpha_s$. One may therefore assume that the dominant QCD effects are included in the meson physics and consider a simple model of quarks and mesons only. As one evolves to scales below $k_{\chi SB}$ the Yukawa coupling decreases whereas α_s increases. Of course, getting closer to Λ_{QCD} it is no longer justified to neglect the QCD effects which go beyond the dynamics of effective meson degrees of freedom. On the other hand, the final IR value of the Yukawa coupling h is fixed by the typical values of constituent quark masses $M_q \simeq 350\,\mathrm{MeV}$ to be $h^2/(4\pi) \simeq 4.5$. One may therefore speculate that the domination of the Yukawa interaction persists down to scales $k \simeq M_q$ at which the quarks decouple from the evolution of the mesonic degrees of freedom altogether due to their mass. Of course, details of the gluonic interactions are expected to be crucial for an understanding of quark and gluon confinement. Strong interaction effects may dramatically change the momentum dependence of the quark n–point functions for k around Λ_{QCD}. Yet, as long as one is only interested in the dynamics of the mesons one is led to expect that these effects are quantitatively not too important. Because of the effective decoupling of the quarks and therefore the whole colored sector the details of confinement have only little influence on the mesonic flow equations for $k \lesssim \Lambda_{\mathrm{QCD}}$. We conclude that there are good prospects that the meson physics can be described by an effective action for mesons and quarks for $k < k_\Phi$. The main part of the work presented here is concerned with this effective quark meson model.

In order to obtain this effective action at the compositeness scale k_Φ from short distance QCD two steps have to be carried out. In a first step one computes at the scale $k_p \simeq 1.5\,\mathrm{GeV}$ an effective action involving only quarks. This step integrates out the gluon degrees of freedom in a "quenched approximation". More precisely, one solves a truncated flow equation for QCD with quark and gluon degrees of freedom in presence of an effective infrared cutoff $k_p \simeq 1.5\,\mathrm{GeV}$ in the quark propagators. The exact flow equation to be used for this purpose is obtained by lowering the infrared cutoff R_k for the gluons to zero while keeping the one for the quarks fixed. Subsequently, the gluons are eliminated by solving the field equations for the gluon fields as functionals of the quarks. This will result in a non–trivial momentum dependence of the quark propagator and effective non–local four and higher quark interactions. Because of the infrared cutoff k_p the resulting effective action for the quarks resembles closely the one for heavy quarks (at least for Euclidean momenta). The dominant effect is the appearance of an effective quark potential (similar to the one for the charm quark) which describes the effective four–quark interactions. For the effective quark action at k_p we only retain this four–quark interaction in addition to the two–point function, while neglecting n–point functions involving six and more quarks.

For typical momenta larger than $\Lambda_{\rm QCD}$ a reliable computation of the effective quark action should be possible by using in the quark–gluon flow equation a relatively simple truncation. The result[18] for the Fourier transform of the potential $V(q^2)$ is shown in figure 1. (See ref[18] for the relation between the four–quark interaction and the heavy quark potential which involves a rescaling in dependence on k_p.) A measure for the truncation uncertainties is the parameter α_* which corresponds to the value to which an appropriately defined running strong coupling α_s evolves for $k \to 0$. We see that these uncertainties affect principally the low–q^2 region. For high values of q^2 the potential is very close to the perturbative two–loop potential whereas for intermediate q^2 relevant for quarkonium spectra it is quite close to phenomenologically acceptable potentials (e.g. the Richardson potential[38]). The inverse quark propagator is found in this computation to remain very well approximated by the simple classical momentum dependence $\not{q}$.

In the second step one has to lower the infrared cutoff in the effective non–local quark model in order to extrapolate from k_p to k_Φ. This task can be carried out by means of the exact flow equation for quarks only, starting at k_p with an initial value $\Gamma_{k_p}[\psi]$ as obtained after integrating out the gluons. For fermions the trace in Eq.(11) has to be replaced by a supertrace in order to account for the minus sign related to Grassmann variables[10]. A first investigation in this direction[33] has used a truncation with a chirally invariant four quark interaction whose most general momentum dependence was retained

$$
\begin{aligned}
\Gamma_k =& \int \frac{d^4 p}{(2\pi)^4} \overline{\psi}^i_a(p) Z_{\psi,k}(p) \left[\not{p}\, \delta^{ab} + m^{ab}(p)\gamma_5 + i\tilde{m}^{ab}(p) \right] \psi_{ib}(p) \\
&+ \frac{1}{2} \int \left(\prod_{l=1}^{4} \frac{d^4 p_l}{(2\pi)^4} \right) (2\pi)^4\, \delta(p_1 + p_2 - p_3 - p_4) \\
&\times \lambda_k^{(\psi)}(p_1,p_2,p_3,p_4) \left\{ \left[\overline{\psi}^i_a(-p_1)\psi_i^b(p_2) \right] \left[\overline{\psi}^j_b(p_4)\psi_j^a(-p_3) \right] \right. \\
&\qquad \left. - \left[\overline{\psi}^i_a(-p_1)\gamma_5\psi_i^b(p_2) \right] \left[\overline{\psi}^j_b(p_4)\gamma_5\psi_j^a(-p_3) \right] \right\} . \qquad (24)
\end{aligned}
$$

Here i,j run from one to N_c which is the number of quark colors. The indices a,b label the different light quark flavors and run from 1 to N. The matrices m and $\tilde{m}$ are hermitian and $m + i\tilde{m}\gamma_5$ forms therefore the most general quark mass matrix. (Our chiral conventions[10] where the hermitean part of the mass matrix is multiplied by γ_5 may be somewhat unusual but they are quite convenient for Euclidean calculations.) The ansatz Eq.(24) does not correspond to the most general chirally invariant four–quark interaction. It neglects similar interactions in the ρ–meson and pomeron channels which are also obtained from a Fierz transformation of the heavy quark potential[16]. With $V(q^2)$ the heavy quark potential in a Fourier representation, the initial value at $k_p = 1.5\,\mathrm{GeV}$ was taken as ($\hat{Z}_{\psi,k} = Z_{\psi,k}(p^2 = -k_p^2)$)

$$
\lambda_{k_p}^{(\psi)}(p_1,p_2,p_3,p_4)\hat{Z}_{\psi,k_p}^{-2} = \frac{1}{2}V((p_1-p_3)^2) = \frac{2\pi\alpha_s}{(p_1-p_3)^2} + \frac{8\pi\lambda}{((p_1-p_3)^2)^2} . \qquad (25)
$$

This corresponds to an approximation by a one gluon exchange term $\sim \alpha_s(k_p)$ and a string tension $\lambda \simeq 0.18\,\mathrm{GeV}^2$ and is in reasonable agreement with the form computed recently[18] from the solution of flow equations (see fig. 1). In the simplified

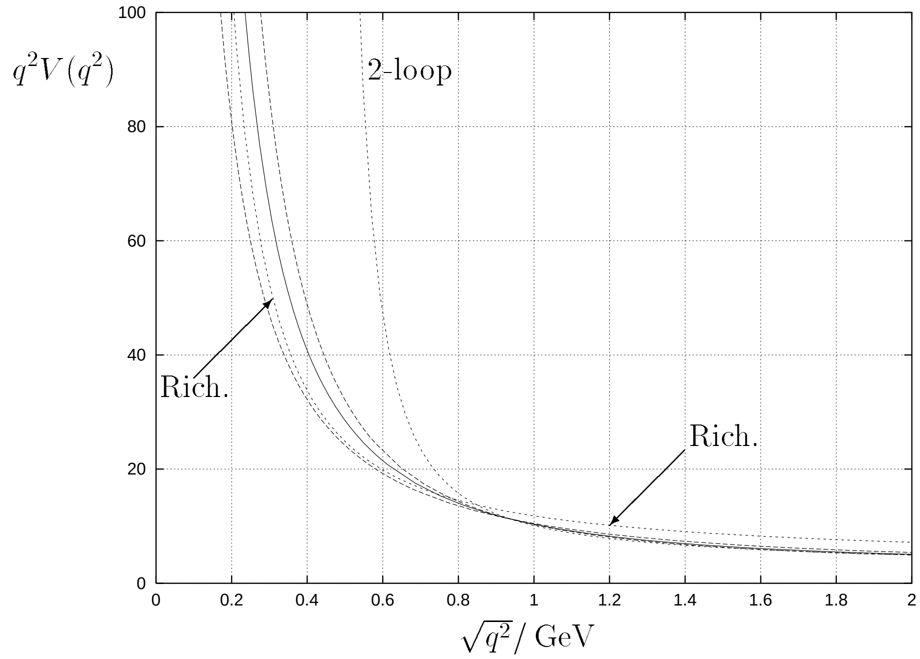

Figure 1. Heavy quark potential for different values of $\alpha_\star$. The solid line corresponds to $\alpha_\star = 1.5$ whereas the dashed lines are for $\alpha_\star = 1$ (lower dashed line) and $\alpha_\star = 2$ (upper dashed line). Also shown are the two loop potential and the Richardson fit as dotted lines.

ansatz Eq.(25) the string tension introduces a second scale in addition to k_p and it becomes clear that the incorporation of gluon fluctuations is a crucial ingredient for the emergence of mesonic bound states. For a more precise treatment[18] of the four–quark interaction at the scale k_Φ this second scale is set by the running of α_s or Λ_{QCD}.

The evolution equation for the function $\lambda_k^{(\psi)}$ for $k < k_p$ can be derived from the fermionic version of Eq.(11) and the truncation Eq.(24). Since $\lambda_k^{(\psi)}$ depends on six independent momentum invariants it is a partial differential equation for a function depending on seven variables and has to be solved numerically[33]. The "initial value" Eq.(25) corresponds to the t–channel exchange of a "dressed" colored gluonic state and it is by far not clear that the evolution of $\lambda_k^{(\psi)}$ will lead at lower scales to a momentum dependence representing the exchange of colorless mesonic bound states. Yet, at the compositeness scale

$$k_\Phi \simeq 630\,\mathrm{MeV} \tag{26}$$

one finds an approximate factorization

$$\lambda_{k_\Phi}^{(\psi)}(p_1, p_2, p_3, p_4) = g(p_1, p_2)\tilde{G}(s)g(p_3, p_4) + \ldots \tag{27}$$

which indicates the formation of mesonic bound states. Here $g(p_1, p_2)$ denotes the amputated Bethe–Salpeter wave function and $\tilde{G}(s)$ is the mesonic bound state propagator displaying a pole–like structure in the s–channel if it is continued to negative $s = (p_1 + p_2)^2$. The dots indicate the part of $\lambda_k^{(\psi)}$ which does not factorize and which will be neglected in the following. In the limit where the momentum dependence of g and $\tilde{G}$ is neglected we recover the four–quark interaction of the Nambu–Jona-Lasinio model[39, 40]. It is therefore not surprising that our description of the dynamics for $k < k_\Phi$ will parallel certain aspects of other investigations of this model, even though we are not bound to the approximations used typically in such studies (large–N_c expansion, perturbative renormalization group, etc.).

It is clear that for scales $k \lesssim k_\Phi$ a description of strong interaction physics in terms of quark fields alone would be rather inefficient. Finding physically reasonable truncations of the effective average action should be much easier once composite fields for the mesons are introduced. The exact renormalization group equation can indeed be supplemented by an exact formalism for the introduction of composite field variables or, more generally, a change of variables[33]. For our purpose, this amounts in practice to inserting at the scale k_Φ the identities

$$
\begin{aligned}
1 &= \text{const} \int \mathcal{D}\sigma_A \\
&\times \exp\left\{ -\operatorname{tr}\left(\sigma_A^\dagger - K_A^\dagger \tilde{G} - m_A^\dagger - \mathcal{O}^\dagger \tilde{G}\right) \frac{1}{2\tilde{G}} \left(\sigma_A - \tilde{G}K_A - m_A - \tilde{G}\mathcal{O}\right)\right\} \\
1 &= \text{const} \int \mathcal{D}\sigma_H \\
&\times \exp\left\{ -\operatorname{tr}\left(\sigma_H^\dagger - K_H^\dagger \tilde{G} - m_H^\dagger - \mathcal{O}^{(5)\dagger} \tilde{G}\right) \frac{1}{2\tilde{G}} \left(\sigma_H - \tilde{G}K_H - m_H - \tilde{G}\mathcal{O}^{(5)}\right)\right\}
\end{aligned}
\tag{28}
$$

into the functional integral which formally defines the quark effective average action. Here we have used the shorthand notation $\operatorname{tr} A^\dagger G B \equiv \int \frac{d^d q}{(2\pi)^d} A_a^*(q) G^{ab}(q) B_b(q)$, and $K_{A,H}$ are sources for the collective fields $\sigma_{A,H}$ which correspond in turn to the anti-hermitian and hermitian parts of the meson field Φ. They are associated to the fermion bilinear operators $\mathcal{O}[\psi]$, $\mathcal{O}^{(5)}[\psi]$ whose Fourier components read

$$
\begin{aligned}
\mathcal{O}^a{}_b(q) &= -i \int \frac{d^4 p}{(2\pi)^4} g(-p, p+q) \overline{\psi}^a(p) \psi_b(p+q) \\
\mathcal{O}^{(5)a}{}_b(q) &= - \int \frac{d^4 p}{(2\pi)^4} g(-p, p+q) \overline{\psi}^a(p) \gamma_5 \psi_b(p+q) \ .
\end{aligned}
\tag{29}
$$

The choice of $g(-p, p+q)$ as the bound state wave function renormalization and of $\tilde{G}(q)$ as its propagator guarantees that the four–quark interaction contained in Eq.(28) cancels the dominant factorizing part of the QCD–induced non–local four–quark interaction Eqs.(24), (27). In addition, one may choose

$$
\begin{aligned}
m_{Hab}^T &= m_{ab}(0) g^{-1}(0,0) Z_{\psi,k_\Phi}(0) \\
m_{Aab}^T &= \tilde{m}_{ab}(0) g^{-1}(0,0) Z_{\psi,k_\Phi}(0)
\end{aligned}
\tag{30}
$$

such that the explicit quark mass term cancels out for $q = 0$. The remaining quark bilinear is $\sim m(q) - m(0) Z_{\psi,k_\Phi}(0) g(-q,q)/[Z_{\psi,k_\Phi}(q) g(0,0)]$. It vanishes for zero momentum and will be neglected in the following. Without loss of generality we can take m real and diagonal and $\tilde{m} = 0$.

In consequence, we have replaced at the scale k_Φ the effective quark action Eq.(24) with Eq.(27) by an effective quark meson action given by

$$
\begin{aligned}
\hat{\Gamma}_k &= \Gamma_k - \frac{1}{2} \int d^4 x \operatorname{tr}\left(\Phi^\dagger \jmath + \jmath^\dagger \Phi\right) \\
\Gamma_k &= \int d^4 x U_k(\Phi, \Phi^\dagger) + \int \frac{d^4 q}{(2\pi)^d} \Bigg\{ Z_{\Phi,k}(q) q^2 \operatorname{tr}\left[\Phi^\dagger(q)\Phi(q)\right] + Z_{\psi,k}(q) \overline{\psi}_a(q) \gamma^\mu q_\mu \psi^a(q) \\
&+ \int \frac{d^4 p}{(2\pi)^d} \overline{h}_k(-q, q-p) \overline{\psi}^a(q) \left(\frac{1+\gamma_5}{2} \Phi_{ab}(p) - \frac{1-\gamma_5}{2} \Phi_{ab}^\dagger(-p)\right) \psi^b(q-p) \Bigg\} \ .
\end{aligned}
\tag{31}
$$

At the scale k_Φ the inverse scalar propagator is related to $\tilde{G}(q)$ in Eq.(27) by

$$
\tilde{G}^{-1}(q^2) = 2\overline{m}_{k_\Phi}^2 + 2 Z_{\Phi,k_\Phi}(q) q^2 \ . \tag{32}
$$

This fixes the term in U_{k_Φ} which is quadratic in Φ to be positive, $U_{k_\Phi} = \overline{m}^2_{k_\Phi}\,\mathrm{tr}\,\Phi^\dagger\Phi + \ldots$. The higher order terms in U_{k_Φ} cannot be determined in the approximation Eq.(24) since they correspond to terms involving six or more quark fields. The initial value of the Yukawa coupling corresponds to the "quark wave function in the meson" in Eq.(27), i.e.

$$\overline{h}_{k_\Phi}(-q, q-p) = g(-q, q-p) \tag{33}$$

which can be normalized with $\overline{h}_{k_\Phi}(0,0) = g(0,0) = 1$. We observe that the explicit chiral symmetry breaking from non–vanishing current quark masses appears now in the form of a meson source term with

$$\jmath = 2\overline{m}^2_{k_\Phi} Z_{\psi,k_\Phi}(0) g^{-1}(0,0)\,(m_{ab} + i\tilde{m}_{ab}) = 2Z_{\psi,k_\Phi}\overline{m}^2_{k_\Phi}\mathrm{diag}(m_u, m_d, m_s)\;. \tag{34}$$

This induces a non–vanishing $\langle\Phi\rangle$ and an effective quark mass M_q through the Yukawa coupling. We note that the current quark mass m_q and the constituent quark mass $M_q \sim \overline{h}_k\langle\Phi\rangle$ are identical at the scale k_Φ. (By solving the field equation for Φ as a functional of $\overline{\psi}$, ψ (with $U_k = \overline{m}^2_k\,\mathrm{tr}\,\Phi^\dagger\Phi$) one recovers from Eq.(31) the effective quark action Eq.(24). For a generalization beyond the approximation of a four–quark interaction or a quadratic potential see ref[52].) Spontaneous chiral symmetry breaking can be described in this language by a non–vanishing $\langle\Phi\rangle$ in the limit $\jmath \to 0$. Because of spontaneous chiral symmetry breaking the constituent quark mass M_q can differ from zero even for $m_q = 0$. It is a nice feature of our formalism that it provides for a unified description of the concepts of the current and the constituent quark masses. As long as the effective average potential U_k has a unique minimum at $\Phi = 0$ there is simply no difference between the two. The running of the current quark mass in the pure quark model should be equivalent in the quark meson language to the running of $\overline{h}_k\langle\Phi\rangle(k)$. (A verification of this property would actually provide a good check for the truncation errors.) Nevertheless, the formalism is now adapted to account for the quark mass contribution from chiral symmetry breaking since the absolute minimum of U_k may be far from the perturbative one for small k. We also note that Γ_k in Eq.(31) is chirally invariant. The explicit chiral symmetry breaking in $\hat{\Gamma}_k$ appears only in the form of a linear source term which is independent of k and does not affect the flow of Γ_k. The flow equation for Γ_k therefore respects chiral symmetry even in the presence of quark masses. This leads to a considerable simplification.

At the scale k_Φ the propagator $\tilde{G}$ and the wave function $g(-q, q-p)$ should be optimized for a most complete elimination of terms quartic in the quark fields. In the present context we will, however, neglect the momentum dependence of $Z_{\psi,k}$, $Z_{\Phi,k}$ and $\overline{h}_k$. The mass $\overline{m}_{k_\Phi}$ was found in[33] for the simple truncation Eq.(24) with $Z_{\psi,k_\Phi} = 1$, $m = \tilde{m} = 0$ to be $\overline{m}_{k_\Phi} \simeq 120\,\mathrm{MeV}$. In view of the possible large truncation errors we will take this only as an order of magnitude estimate. Below we will consider the range $\overline{m}_{k_\Phi} = (45 - 120)\,\mathrm{MeV}$ for which chiral symmetry breaking can be obtained in a two flavor model. Furthermore, we will assume, as usually done in large–N_c computations within the NJL–model, that $Z_{\Phi,k_\Phi} \equiv Z_{\Phi,k_\Phi}(q=0) \ll 1$. The quark wave function renormalization $Z_{\psi,k} \equiv Z_{\psi,k}(q=0)$ is set to one at the scale k_Φ for convenience. For $k < k_\Phi$ we will therefore study an effective action for quarks and mesons in the truncation

$$\begin{aligned}\Gamma_k = \int d^4x \Big\{ & Z_{\psi,k}\overline{\psi}_a i\partial\!\!\!/\,\psi^a + Z_{\Phi,k}\,\mathrm{tr}\left[\partial_\mu\Phi^\dagger\partial^\mu\Phi\right] + U_k(\Phi,\Phi^\dagger) \\ & + \overline{h}_k\overline{\psi}^a\left(\frac{1+\gamma_5}{2}\Phi_{ab} - \frac{1-\gamma_5}{2}(\Phi^\dagger)_{ab}\right)\psi^b\Big\}\end{aligned} \tag{35}$$

with compositeness conditions

$$
\begin{aligned}
U_{k_\Phi}(\Phi,\Phi^\dagger) &= \overline{m}^2_{k_\Phi}\,\mathrm{tr}\,\Phi^\dagger\Phi - \frac{1}{2}\overline{\nu}_{k_\Phi}\left(\det\Phi + \det\Phi^\dagger\right) \\
&+ \frac{1}{2}\overline{\lambda}_{1,k_\Phi}\left(\mathrm{tr}\,\Phi^\dagger\Phi\right)^2 + \frac{N-1}{4}\overline{\lambda}_{2,k_\Phi}\,\mathrm{tr}\left(\Phi^\dagger\Phi - \frac{1}{N}\,\mathrm{tr}\,\Phi^\dagger\Phi\right)^2 + \ldots \\
\overline{m}^2_{k_\Phi} &\equiv \frac{1}{2\tilde{G}(0)} \simeq (45\,\mathrm{MeV})^2 - (120\,\mathrm{MeV})^2 \\
\overline{h}_{k_\Phi} &= Z_{\psi,k_\Phi} = 1 \\
Z_{\Phi,k_\Phi} &\ll 1\,. \qquad (36)
\end{aligned}
$$

As a consequence, the initial value of the renormalized Yukawa coupling which is given by $h_{k_\Phi} = \overline{h}_{k_\Phi} Z^{-1}_{\psi,k_\Phi} Z^{-1/2}_{\Phi,k_\Phi}$ is large! Note that we have included in the potential an explicit $U_A(1)$ breaking term[‡] $\sim \overline{\nu}_k$ which mimics the effect of the chiral anomaly of QCD to leading order in an expansion of the effective potential in powers of Φ. Because of the infrared stability of the evolution of Γ_k which will be discussed below the precise form of the potential, i.e. the values of the quartic couplings $\overline{\lambda}_{i,k_\Phi}$ and so on, will turn out to be unimportant.

We have refrained here for simplicity from considering four quark operators with vector and pseudo–vector spin structure. Their inclusion is straightforward and would lead to vector and pseudo–vector mesons in the effective action Eq.(35). We will concentrate first on two flavors and consider only the two limiting cases $\overline{\nu}_k = 0$ and $\overline{\nu}_k \to \infty$. We also omit first the explicit quark masses and study the chiral limit $\jmath = 0$. Because of the positive mass term $\overline{m}^2_{k_\Phi}$ one has at the scale k_Φ a vanishing expectation value $\langle\Phi\rangle = 0$ (for $\jmath = 0$). There is no spontaneous chiral symmetry breaking at the compositeness scale. This means that the mesonic bound states at k_Φ and somewhat below are not directly connected to chiral symmetry breaking.

The question remains how chiral symmetry is broken. We will try to answer it by following the evolution of the effective potential U_k from k_Φ to lower scales using the exact renormalization group method outlined above with the compositeness conditions Eq.(36) defining the initial values. In this context it is important that the formalism for composite fields[33] also induces an infrared cutoff in the meson propagator. The flow equations are therefore exactly of the form Eq.(11) (except for the supertrace), with quarks and mesons treated on an equal footing. In fact, one would expect that the large renormalized Yukawa coupling will rapidly drive the scalar mass term to negative values as the IR cutoff k is lowered[10]. This will then finally lead to a potential minimum away from the origin at some scale $k_{\chi\mathrm{SB}} < k_\Phi$ such that $\langle\Phi\rangle \neq 0$. The ultimate goal of such a procedure, besides from establishing the onset of chiral symmetry breaking, would be to extract phenomenological quantities, like f_π or meson masses, which can be computed in a straightforward manner from Γ_k in the IR limit $k \to 0$.

At first sight, a reliable computation of $\Gamma_{k\to 0}$ seems a very difficult task. Without a truncation Γ_k is described by an infinite number of parameters (couplings, wave function renormalizations, etc.) as can be seen if Γ_k is expanded in powers of fields and derivatives. For instance, the pseudoscalar and scalar meson masses are obtained as the poles of the exact propagator, $\lim_{k\to 0}\Gamma^{(2)}_k(q)|_{\Phi=\langle\Phi\rangle}$, which receives formally contributions from terms in Γ_k with arbitrarily high powers of derivatives and the expectation value σ_0. Realistic nonperturbative truncations of Γ_k which reduce the problem to a manageable size are crucial. We will argue in the following that there may be a twofold solution to this problem:

---

‡The anomaly term in the fermionic effective average action has been computed in[41].

- Due to an IR fixed point structure of the flow equations in the symmetric regime, i.e. for $k_{\chi SB} < k < k_\Phi$, the values of many parameters of Γ_k for $k \to 0$ will be approximately independent of their initial values at the compositeness scale k_Φ. For small enough Z_{Φ,k_Φ} only a few relevant parameters ($\overline{m}^2_{k_\Phi}$, $\overline{\nu}_{k_\Phi}$) need to be computed accurately from QCD. They can alternatively be determined from phenomenology.

- One can show that physical observables like meson masses, decay constants, etc., can be expanded in powers of the quark masses within the linear meson model[42, 43, 44]. This is similar to the way it is usually done in chiral perturbation theory[36]. To a given finite order of this expansion only a finite number of terms of a simultaneous expansion of Γ_k in powers of derivatives and Φ are required if the expansion point is chosen properly.

In combination, these two results open the possibility for a perhaps unexpected degree of predictive power within the linear meson model.

We wish to stress, though, that a perturbative treatment of the model at hand, e.g., using perturbative RG techniques, cannot be expected to yield reliable results. The renormalized Yukawa coupling is expected to be large at the scale k_Φ. Even the IR value of h is still relatively big

$$\lim_{k\to 0} h = \frac{2M_q}{f_\pi} \simeq 7.5 \tag{37}$$

and h increases with increasing k. The dynamics of the linear meson model is therefore clearly nonperturbative for all scales $k \leq k_\Phi$.

FLOW EQUATIONS FOR THE LINEAR QUARK MESON MODEL

We will next turn to the ERGE analysis of the linear meson model which was introduced in the last section[§]. In a first approach we will attack the problem at hand by truncating Γ_k in such a way that it contains all perturbatively relevant and marginal operators, i.e. those with canonical dimensions. This has the advantage that the flow of a small number of couplings permits quantitative insight into the relevant mechanisms, e.g., of chiral symmetry breaking. More quantitative precision will be obtained once we generalize our truncation (see below) for the $O(4)$–model by allowing for the most general effective average potential U_k. The effective potential U_k is a function of only four $SU_L(N) \times SU_R(N)$ invariants for $N = 3$:

$$\begin{aligned}
\rho &= \mathrm{tr}\, \Phi^\dagger \Phi \\
\tau_2 &= \frac{N}{N-1} \mathrm{tr} \left(\Phi^\dagger \Phi - \frac{1}{N} \rho \right)^2 \\
\tau_3 &= \mathrm{tr} \left(\Phi^\dagger \Phi - \frac{1}{N} \rho \right)^3 \\
\xi &= \det \Phi + \det \Phi^\dagger \; .
\end{aligned} \tag{38}$$

The invariant τ_3 is only independent for $N \geq 3$. For $N = 2$ it can be eliminated by a suitable combination of τ_2 and ρ. The additional $U_A(1)$ breaking invariant $\omega = i(\det \Phi - \det \Phi^\dagger)$ is $\mathcal{CP}$ violating and may therefore appear only quadratically in U_k. It is

[§]For a study of chiral symmetry breaking in QED using related exact renormalization group techniques see ref[45].

straightforward to see that ω^2 is expressible in terms of the invariants Eq.(38). We may expand U_k as a function of these invariants around its minimum, i.e. $\rho = \rho_0 \equiv N\overline{\sigma}_0^2$, $\xi = \xi_0 = 2\overline{\sigma}_0^N$ and $\tau_2 = \tau_3 = 0$ where

$$\overline{\sigma}_0 \equiv \frac{1}{N}\,\mathrm{tr}\,\langle\Phi\rangle\ . \tag{39}$$

The expansion coefficients are the k–dependent couplings of the model. In our first version we only keep couplings of canonical dimension $d_c \leq 4$. This yields in the chirally symmetric regime, i.e., for $k_{\chi\mathrm{SB}} \leq k \leq k_\Phi$ where $\overline{\sigma}_0 = 0$

$$U_k = \overline{m}_k^2\rho + \frac{1}{2}\overline{\lambda}_{1,k}\rho^2 + \frac{N-1}{4}\overline{\lambda}_{2,k}\tau_2 - \frac{1}{2}\overline{\nu}_k\xi \tag{40}$$

whereas in the SSB regime for $k \leq k_{\chi\mathrm{SB}}$ we have

$$U_k = \frac{1}{2}\overline{\lambda}_{1,k}\left[\rho - N\overline{\sigma}_{0,k}^2\right]^2 + \frac{N-1}{4}\overline{\lambda}_{2,k}\tau_2 + \frac{1}{2}\overline{\nu}_k\left[\overline{\sigma}_{0,k}^{N-2}\rho - \xi\right]\ . \tag{41}$$

Before continuing to compute the nonperturbative beta functions for these couplings it is worthwhile to pause here and emphasize that naively (perturbatively) irrelevant operators can by no means always be neglected. The most prominent example for this is QCD itself. It is the very assumption of our treatment of chiral symmetry breaking (substantiated by the results of[33]) that the momentum dependence of the coupling constants of some six–dimensional quark operators $(\overline{\psi}\psi)^2$ develop poles in the s–channel indicating the formation of mesonic bound states. On the other hand, it is quite natural to assume that Φ^6 or Φ^8 operators are not really necessary to understand the properties of the potential in a neighborhood around its minimum. Yet, truncating higher dimensional operators does not imply the assumption that the corresponding coupling constants are small. In fact, this could only be expected as long as the relevant and marginal couplings are small as well. What is required, though, is that their *influence* on the evolution of those couplings kept in the truncation, for instance, the set of equations Eq.(43) below, is small. A comparison with the results of the later sections for the full potential U_k (i.e., including arbitrarily many couplings in the formal expansion) will provide a good check for the validity of this assumption. In this context it is perhaps also interesting to note that the truncation Eq.(35) includes the known one–loop beta functions of a small coupling expansion as well as the leading order result of the large–N_c expansion of the $U_L(N) \times U_R(N)$ model[46]. This should provide at least some minimal control over this truncation, even though we believe that our results are significantly more accurate.

Inserting the truncation Eqs.(35), (40), (41) into Eq.(11) reduces this functional differential equation for infinitely many variables to a finite set of ordinary differential equations. This yields, in particular, the beta functions for the couplings $\overline{\lambda}_{1,k}$, $\overline{\lambda}_{2,k}$, $\overline{\nu}_k$ and $\overline{m}_k^2$ or $\overline{\sigma}_{0,k}$. Details of the calculation can be found in[47]. We will refrain here from presenting the full set of flow equations but rather illustrate the main results with a few examples. Defining dimensionless renormalized VEV and coupling constants

$$\begin{aligned}
\kappa &= Z_{\Phi,k}N\overline{\sigma}_{0,k}^2k^{-2}\\
h^2 &= \overline{h}_k^2 Z_{\Phi,k}^{-1}Z_{\psi,k}^{-2}\\
\lambda_i &= \overline{\lambda}_{i,k}Z_{\Phi,k}^{-2}\,;\quad i=1,2\\
\nu &= \overline{\nu}_k Z_{\Phi,k}^{-\frac{N}{2}}k^{N-4}
\end{aligned} \tag{42}$$

one finds, e.g., for the spontaneous symmetry breaking (SSB) regime and $\overline{\nu}_k = 0$

$$
\begin{aligned}
\frac{d}{dt}\kappa &= -(2+\eta_\Phi)\kappa + \frac{1}{16\pi^2}\Big\{ N^2 l_1^4(0;\eta_\Phi) + 3 l_1^4(2\lambda_1\kappa;\eta_\Phi) \\
&+ (N^2-1)\left[1+\frac{\lambda_2}{\lambda_1}\right] l_1^4(\lambda_2\kappa;\eta_\Phi) - 4N_c\frac{h^2}{\lambda_1} l_1^{(F)4}(\frac{1}{N}h^2\kappa;\eta_\psi)\Big\} \\
\frac{d}{dt}\lambda_1 &= 2\eta_\Phi\lambda_1 + \frac{1}{16\pi^2}\Big\{ N^2\lambda_1^2 l_2^4(0;\eta_\Phi) + 9\lambda_1^2 l_2^4(2\lambda_1\kappa;\eta_\Phi) \\
&+ (N^2-1)\left[\lambda_1+\lambda_2\right]^2 l_2^4(\lambda_2\kappa;\eta_\Phi) - 4\frac{N_c}{N} h^4 l_2^{(F)4}(\frac{1}{N}h^2\kappa;\eta_\psi)\Big\} \\
\frac{d}{dt}\lambda_2 &= 2\eta_\Phi\lambda_2 + \frac{1}{16\pi^2}\Big\{ \frac{N^2}{4}\lambda_2^2 l_2^4(0;\eta_\Phi) + \frac{9}{4}(N^2-4)\lambda_2^2 l_2^4(\lambda_2\kappa;\eta_\Phi) \\
&- \frac{1}{2}N^2\lambda_2^2 l_{1,1}^4(0,\lambda_2\kappa;\eta_\Phi) + 3[\lambda_2+4\lambda_1]\lambda_2 l_{1,1}^4(2\lambda_1\kappa,\lambda_2\kappa;\eta_\Phi) \\
&- 8\frac{N_c}{N} h^4 l_2^{(F)4}(\frac{1}{N}h^2\kappa;\eta_\psi)\Big\} \\
\frac{d}{dt}h^2 &= \left[d-4+2\eta_\psi+\eta_\Phi\right] h^2 - \frac{4}{N} v_d h^4 \Big\{ N^2 l_{1,1}^{(FB)d}(\frac{1}{N}\kappa h^2, 0;\eta_\psi,\eta_\Phi) \\
&- (N^2-1) l_{1,1}^{(FB)d}(\frac{1}{N}\kappa h^2, \kappa\lambda_2;\eta_\psi,\eta_\Phi) \\
&- l_{1,1}^{(FB)d}(\frac{1}{N}\kappa h^2, 2\kappa\lambda_1;\eta_\psi,\eta_\Phi)\Big\}
\end{aligned}
\tag{43}
$$

Here $\eta_\Phi = -\frac{d}{dt}\ln Z_{\Phi,k}$, $\eta_\psi = -\frac{d}{dt}\ln Z_{\psi,k}$ are the meson and quark anomalous dimensions, respectively[47]. The symbols l_n^d, l_{n_1,n_2}^d and $l_n^{(F)d}$ denote bosonic and fermionic mass threshold functions, respectively, which are defined in[47]. They describe the decoupling of massive modes and provide an important nonperturbative ingredient. For instance, the bosonic threshold functions

$$
l_n^d(w;\eta_\Phi) = \frac{n+\delta_{n,0}}{4} v_d^{-1} k^{2n-d} \int \frac{d^d q}{(2\pi)^d} \frac{1}{Z_{\Phi,k}} \frac{\partial R_k}{\partial t} \frac{1}{\left[P(q^2)+k^2 w\right]^{n+1}}
\tag{44}
$$

involve the inverse average propagator $P(q^2) = q^2 + Z_{\Phi,k}^{-1} R_k(q^2)$ where the infrared cutoff is manifest. These functions decrease $\sim w^{-(n+1)}$ for $w \gg 1$. Since typically $w = M^2/k^2$ with M a mass of the model, the main effect of the threshold functions is to cut off fluctuations of particles with masses $M^2 \gg k^2$. Once the scale k is changed below a certain mass threshold, the corresponding particle no longer contributes to the evolution and decouples smoothly.

Within our truncation the beta functions Eq.(43) for the dimensionless couplings look almost the same as in one–loop perturbation theory. There are, however, two major new ingredients which are crucial for our approach: First, there is a new equation for the running of the mass term in the symmetric regime or for the running of the potential minimum in the regime with spontaneous symmetry breaking. This equation is related to the quadratic divergence of the mass term in perturbation theory and does not appear in the Callan–Symanzik[48] or Coleman–Weinberg[49] treatment of the renormalization group. Obviously, these equations are the key for a study of the onset of spontaneous chiral symmetry breaking as k is lowered from k_Φ to zero. Second, the most important nonperturbative ingredient in the flow equations for the dimensionless Yukawa and scalar couplings is the appearance of effective mass threshold functions like

Eq.(44) which account for the decoupling of modes with masses larger than k. Their form is different for the symmetric regime (massless fermions, massive scalars) or the regime with spontaneous symmetry breaking (massive fermions, massless Goldstone bosons). Without the inclusion of the threshold effects the running of the couplings would never stop and no sensible limit $k \to 0$ could be obtained because of unphysical infrared divergences. The threshold functions are not arbitrary but have to be computed carefully. The mass terms appearing in these functions involve the dimensionless couplings. Expanding the threshold functions in powers of the mass terms (or the dimensionless couplings) makes their non–perturbative content immediately visible. It is these threshold functions which will make it possible below to use one–loop type formulae for the necessarily nonperturbative computation of the critical behavior of the (effectively) three–dimensional $O(4)$–symmetric scalar model.

THE CHIRAL ANOMALY AND THE $O(4)$–MODEL

We have seen how the mass threshold functions in the flow equations describe the decoupling of heavy modes from the evolution of Γ_k as the IR cutoff k is lowered. In the chiral limit with two massless quark flavors ($N = 2$) the pions are the massless Goldstone bosons. Below, once we will consider the flow of the full effective average potential without resorting to a quartic truncation, we will also consider the more general case of non–vanishing current quark masses. For the time being, the effect of the physical pion mass of $m_\pi \simeq 140\,\mathrm{MeV}$, or equivalently of the two small but non–vanishing current quark masses, can easily be mimicked by stopping the flow of Γ_k at $k = m_\pi$ by hand. This situation changes significantly once the strange quark is included. Now the η and the four K mesons appear as additional massless Goldstone modes in the spectrum. They would artificially drive the running of Γ_k at scales $m_\pi \lesssim k \lesssim 500\,\mathrm{MeV}$ where they should already be decoupled because of their physical masses. It is therefore advisable to focus on the two flavor case $N = 2$ as long as the chiral limit of vanishing current quark masses is considered.

It is straightforward to obtain an estimate of the (renormalized) coupling ν which parameterizes the explicit $U_A(1)$ breaking due to the chiral anomaly. From Eq.(41) we find

$$m^2_{\eta'} = \frac{N}{2}\nu\sigma_0^{N-2} \simeq 1\,\mathrm{GeV} \tag{45}$$

which translates for $N = 2$ for $k \to 0$ into

$$\nu(k \to 0) \simeq 1\,\mathrm{GeV}\ . \tag{46}$$

This suggests that $\nu \to \infty$ can be considered as a realistic limit. An important simplification occurs for $N = 2$ and $\nu \to \infty$, related to the fact that for $N = 2$ the chiral group $SU_L(2) \times SU_R(2)$ is (locally) isomorphic to $O(4)$. Thus, the complex $(\mathbf{2},\mathbf{2})$ representation Φ of $SU_L(2) \times SU_R(2)$ may be decomposed into two vector representations, (σ, π^k) and (η', a^k) of $O(4)$:

$$\Phi = \frac{1}{2}\left(\sigma - i\eta'\right) + \frac{1}{2}\left(a^k + i\pi^k\right)\tau_k\ . \tag{47}$$

For $\nu \to \infty$ the masses of the η' and the a^k diverge and these particles decouple. We are then left with the original $O(4)$ symmetric linear σ–model of Gell–Mann and Levy[50] coupled to quarks. The flow equations of this model have been derived previously[10, 7] for the truncation of the effective action used here. For mere comparison we also consider the opposite limit $\nu \to 0$. Here the η' meson becomes an additional Goldstone boson in the chiral limit which suffers from the same problem as the K and the η in the case $N = 3$. Hence, we may compare the results for two different approximate limits of the effects of the chiral anomaly:

- the $O(4)$ model corresponding to $N = 2$ and $\nu \to \infty$
- the $U_L(2) \times U_R(2)$ model corresponding to $N = 2$ and $\nu = 0$.

For the reasons given above we expect the first situation to be closer to reality. In this case we may imagine that the fluctuations of the kaons, η, η' and the scalar mesons (as well as vector and pseudovector mesons) have been integrated out in order to obtain the initial values of Γ_{k_Φ} — in close analogy to the integration of the gluons for the effective quark action $\Gamma_{k_p}[\psi]$ discussed above. We will keep the initial values of the couplings $\overline{m}^2_{k_\Phi}$, $\overline{\lambda}_{1,k_\Phi}$ and Z_{Φ,k_Φ} as free parameters. Our results should be quantitatively accurate to the extent to which the local polynomial truncation is a good approximation.

INFRARED STABILITY

Eq.(43) and the corresponding set of flow equations for the symmetric regime constitute a coupled system of ordinary differential equations which can be integrated numerically. Similar equations can be computed for the $O(4)$ model where $N = 2$ and the coupling λ_2 is absent. We have neglected in a first step the dependence of all threshold functions appearing in the flow equations on the anomalous dimensions. This dependence will be taken into account below once we abandon the quartic potential approximation. The most important result is that chiral symmetry breaking indeed occurs for a wide range of initial values of the parameters including the presumably realistic case of large renormalized Yukawa coupling and a bare mass $\overline{m}_{k_\Phi}$ of order 100 MeV. A typical evolution of the renormalized meson mass m with k is plotted in fig. 2. Driven by the strong Yukawa coupling, m decreases rapidly and goes through

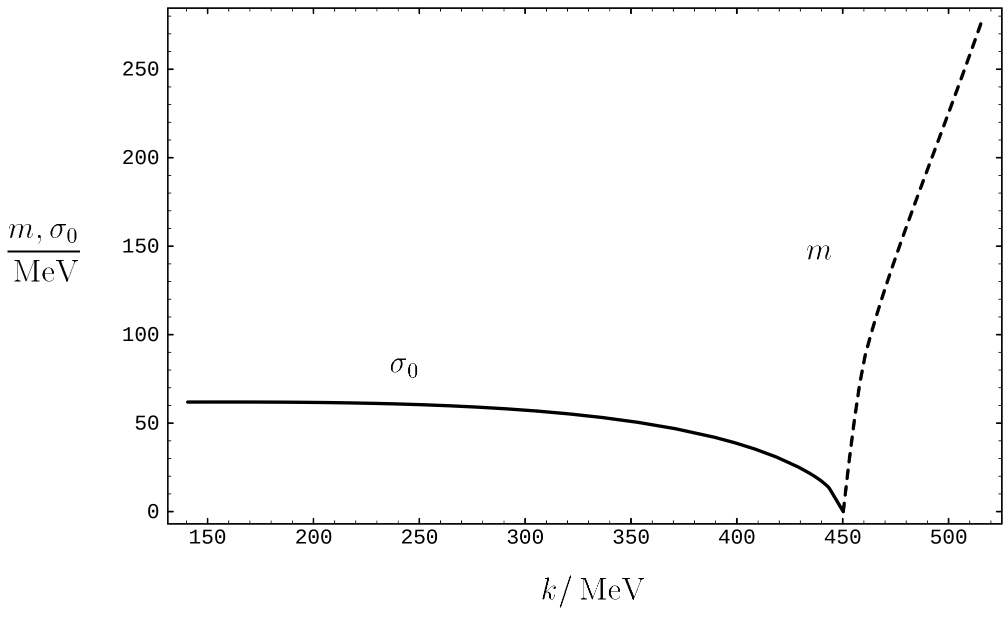

Figure 2. Evolution of the renormalized mass m in the symmetric regime (dashed line) and the vacuum expectation value $\sigma_0 = Z^{1/2}_{\Phi,k}\overline{\sigma}_{0,k}$ of the scalar field in the SSB regime (solid line) as functions of k for the $U_L(2) \times U_R(2)$ model. Initial values at $k = k_\Phi$ are $\lambda_{i,I} = 0$, $h_I^2 = 300$ and $\overline{m}_{k_\Phi} = 63\,\mathrm{MeV}$.

zero at a scale $k_{\chi \mathrm{SB}}$ not far below k_Φ. Here the system enters the SSB regime and a non–vanishing (renormalized) VEV σ_0 for the meson field Φ develops. The evolution of σ_0 with k turns out to be reasonably stable already before scales $k \simeq m_\pi$ where the evolution is stopped. We take this result as an indication that our truncation of the effective action Γ_k leads at least qualitatively to a satisfactory description of chiral symmetry breaking. The reason for the relative stability of the IR behavior of the VEV (and all other couplings) is that the quarks acquire a constituent mass $M_q = h\sigma_0 \simeq 350\,\mathrm{MeV}$ in the SSB regime. As a consequence they decouple once k becomes smaller than M_q and the evolution is then dominantly driven by the massless Goldstone bosons. This is also important in view of potential confinement effects expected to become important for the quark n–point functions for k around $\Lambda_{\mathrm{QCD}} \simeq 200\,\mathrm{MeV}$. Since confinement is not explicitly included in our truncation of Γ_k, one might be worried that such effects could spoil our results completely. Yet, as discussed in some more detail above, only the colored quarks should feel confinement and they are no longer important for the evolution of the meson couplings for k around 200 MeV. One might therefore hope that a precise treatment of confinement is not crucial for this approach to chiral symmetry breaking.

Most importantly, one finds that the system of flow equations exhibits a partial IR fixed point in the symmetric phase. As already pointed out one expects Z_{Φ,k_Φ} to be rather small. In turn, one may assume that, at least for the initial range of running in the symmetric regime the mass parameter $m^2 \sim Z_{\Phi,k}^{-1}$ is large. This means, in particular, that all threshold functions with arguments $\sim m^2$ may be neglected in this regime. As a consequence, the flow equations simplify considerably. We find, for instance, for the $U_L(2) \times U_R(2)$ model

$$
\begin{aligned}
\frac{d}{dt}\tilde{\lambda}_1 &\equiv \frac{d}{dt}\frac{\lambda_1}{h^2} \simeq \frac{N_c}{4\pi^2}h^2\left[\frac{1}{2}\tilde{\lambda}_1 - \frac{1}{N}\right] \\
\frac{d}{dt}\tilde{\lambda}_2 &\equiv \frac{d}{dt}\frac{\lambda_2}{h^2} \simeq \frac{N_c}{4\pi^2}h^2\left[\frac{1}{2}\tilde{\lambda}_2 - \frac{2}{N}\right] \\
\frac{d}{dt}h^2 &\simeq \frac{N_c}{8\pi^2}h^4 \\
\eta_\Phi &\simeq \frac{N_c}{8\pi^2}h^2\ , \quad \eta_\psi \simeq 0\ .
\end{aligned}
\tag{48}
$$

This system possesses an attractive IR fixed point for the quartic scalar self interactions

$$
\tilde{\lambda}_{1*} = \frac{1}{2}\tilde{\lambda}_{2*} = \frac{2}{N}\ . \tag{49}
$$

Furthermore it is exactly soluble[47]. Because of the strong Yukawa coupling the quartic couplings $\tilde{\lambda}_1$ and $\tilde{\lambda}_2$ generally approach their fixed point values rapidly, long before the systems enters the broken phase ($m \to 0$) and the approximation of large m breaks down. In addition, for large initial values h_I^2 the Yukawa coupling at the scale $k_{\chi SB}$ where m vanishes (or becomes small) only depends on the initial value $\overline{m}_{k_\Phi}$. Hence, the system is approximately independent in the IR upon the initial values of λ_1, λ_2 and h^2, the only "relevant" parameter being $\overline{m}_{k_\Phi}$. (Once quark masses and a proper treatment of the chiral anomaly are included for $N = 3$ one expects that m_q and ν are additional relevant parameters. Their values may be fixed by using the masses of π, K and η' as phenomenological input.) In other words, the effective action looses almost all its "memory" in the far IR of where in the UV it came from. This feature of the flow equations leads to a perhaps surprising degree of predictive power. In addition, also the dependence of $f_\pi = 2\sigma_0$ on $\overline{m}_{k_\Phi}$ is not very strong for a large range in $\overline{m}_{k_\Phi}$, as shown in fig. 3. The relevant parameter $\overline{m}_{k_\Phi}$ can be fixed by using the constituent quark mass $M_q \equiv h\sigma_0 \simeq 350\,\mathrm{MeV}$ as a phenomenological input. One obtains for the $O(4)$–model

$$\frac{\overline{m}^2_{k_\Phi}}{k^2_\Phi} \simeq 0.02\ . \tag{50}$$

The resulting value for the decay constant is

$$f_\pi = (91 - 100)\,\mathrm{MeV} \tag{51}$$

for $h_I^2 = 10^4 - 300$. It is striking that this comes close to the real value $f_\pi = 92.4\,\mathrm{MeV}$ but we expect that the uncertainty in the determination of the compositeness scale k_Φ and the truncation errors exceed the influence of the variation of h_I^2. We have furthermore used this result for an estimate of the chiral condensate:

$$\left\langle\overline{\psi}\psi\right\rangle \equiv -\overline{m}^2_{k_\Phi} f_\pi Z^{-1/2}_{\Phi,k=0} A \simeq -(195\,\mathrm{MeV})^3 \tag{52}$$

where the factor $A \simeq 1.7$ accounts for the change of the normalization scale of $\left\langle\overline{\psi}\psi\right\rangle$ from k_Φ to the commonly used value 1 GeV. Our value is in reasonable agreement with results from sum rules[51]. This is non–trivial since not only $\overline{m}_{k_\Phi}$ and f_π enter but also the IR value $Z_{\Phi,k=0}$. Integrating Eq.(48) for η_Φ one finds

$$Z_{\Phi,k} = Z_{\Phi,k_\Phi} + \frac{N_c}{8\pi^2}\ln\frac{k_\Phi}{k}\ . \tag{53}$$

Thus $Z_{\Phi,k}$ will indeed be practically independent of its initial value Z_{Φ,k_Φ} already after some running as long as Z_{Φ,k_Φ} is small compared to 0.01.

The alert reader may have noticed that the beta functions Eq.(48) correspond exactly to those obtained in the one–quark–loop approximation or, in other words, to the leading order in the large–N_c expansion for the Nambu–Jona-Lasinio model[46]. The fixed point Eq.(49) is then nothing but the large–N_c boundary condition on the evolution of λ_1 and λ_2 in this model. Yet, we wish to stress that nowhere we have

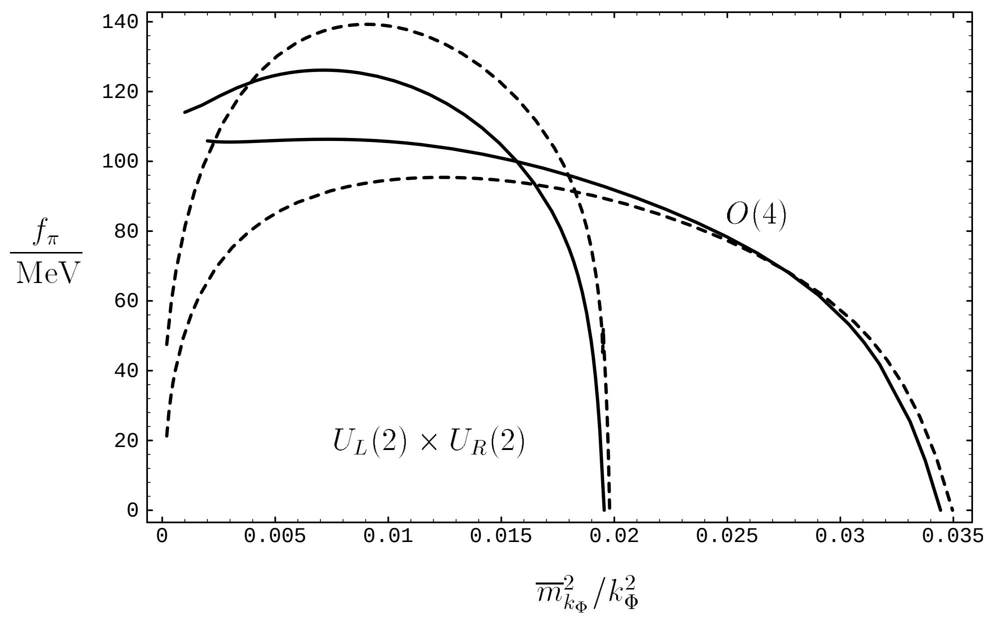

Figure 3. The pion decay constant f_π as a function of $\overline{m}^2_{k_\Phi}/k^2_\Phi$ for $k_\Phi = 630\,\mathrm{MeV}$ and initial values $\lambda_{i,I} = 0$ and $h_I^2 = 300$ (solid line) as well as $h_I^2 = 10^4$ (dashed line).

made the assumption that N_c is a large number. On the contrary, the physical value $N_c = 3$ suggests that the large–N_c expansion should a priori only be trusted on a quantitatively rather crude level. The reason why we expect Eq.(48) to nevertheless give rather reliable results is based on the fact that for small Z_{Φ,k_Φ} all (renormalized) meson masses are much larger than the scale k for the initial part of the running. This implies that the mesons are effectively decoupled and their contribution to the beta functions is negligible leading to the one–quark–loop approximation. Yet, already after some relatively short period of running the renormalized meson masses approach zero and our approximation of neglecting mesonic threshold functions breaks down. Hence, the one–quark–loop approximation is reasonable only for scales close to k_Φ but is bound to become inaccurate around $k_{\chi\mathrm{SB}}$ and in the SSB regime. What is important in our context is not the numerical value of the partial fixed points Eq.(49) but rather their mere existence and the presence of a large coupling h^2 driving the $\tilde{\lambda}_i$ fast towards them. This is enough for the IR values of all couplings to become almost independent of the initial values $\lambda_{i,I}$. Similar features of IR stability are expected if the truncation is enlarged, for instance, to a more general form of the effective potential U_{k_Φ} as will be discussed in the next section.

FLOW EQUATIONS FOR THE SCALAR POTENTIAL

In this and the remaining sections we consider the $O(4)$–symmetric quark meson model without truncating its effective average potential to a polynomial form[52]. A comparison with the results of the last sections will give us a feeling for the size of the errors induced by the quartic truncation used so far. Furthermore, such an approach is well suited for a study of the chiral phase transition close to which the form of the potential deviates substantially from a polynomial.

It is convenient to work with dimensionless and renormalized variables therefore eliminating all explicit k–dependence. With ($t = \ln(k/k_\Phi)$)

$$u(t,\tilde{\rho}) \equiv k^{-d} U_k(\rho) \ , \quad \tilde{\rho} \equiv Z_{\Phi,k} k^{2-d} \rho \tag{54}$$

and using Eq.(35) as a first truncation of the effective average action Γ_k one obtains the flow equation in arbitrary dimensions d

$$\begin{aligned} \frac{\partial}{\partial t} u &= -du + (d-2+\eta_\Phi)\,\tilde{\rho} u' \\ &+ 2v_d \left\{ 3 l_0^d(u';\eta_\Phi) + l_0^d(u'+2\tilde{\rho}u'';\eta_\Phi) - 2^{\frac{d}{2}+1} N_c l_0^{(F)d}(\frac{1}{2}\tilde{\rho}h^2;\eta_\psi) \right\} . \end{aligned} \tag{55}$$

Here $v_d^{-1} \equiv 2^{d+1}\pi^{d/2}\Gamma(d/2)$ and primes denote derivatives with respect to $\tilde{\rho}$. We will always use in the following for the number of quark colors $N_c = 3$. Eq.(55) is a partial differential equation for the effective potential $u(t,\tilde{\rho})$ which has to be supplemented by the flow equation for the Yukawa coupling and expressions for the anomalous dimensions η_Φ, η_ψ. The definition of the threshold functions l_n^d, $l_n^{(F)d}$ can be found in[47].

The dimensionless renormalized expectation value $\kappa \equiv 2k^{2-d} Z_{\Phi,k} \overline{\sigma}_{0,k}^2$, with $\overline{\sigma}_{0,k}$ the k–dependent VEV of Φ, may be computed for each k directly from the condition

$$u'(t,\kappa) = \frac{\jmath}{\sqrt{2\kappa}} k^{-\frac{d+2}{2}} Z_{\Phi,k}^{-1/2} \equiv \epsilon_g \tag{56}$$

where[52]

$$\jmath = 2\overline{m}_{k_\Phi,k}^2 \hat{m} \tag{57}$$

and $\hat{m} = (m_u + m_d)/2$ denotes the average light current quark mass normalized at k_Φ. Note that $\kappa \equiv 0$ in the symmetric regime for vanishing source term. Eq.(56) allows us to follow the flow of κ according to

$$\frac{d}{dt}\kappa = \frac{\kappa}{\epsilon_g + 2\kappa\lambda}\left\{ \left[\eta_\Phi - d - 2\right]\epsilon_g - 2\frac{\partial}{\partial t}u'(t,\kappa)\right\} \tag{58}$$

with $\lambda \equiv u''(t,\kappa)$. We define the Yukawa coupling for $\tilde{\rho} = \kappa$ and its flow equation reads[47]

$$\begin{aligned} \frac{d}{dt}h^2 &= (d - 4 + 2\eta_\psi + \eta_\Phi)\, h^2 - 2v_d h^4 \left\{ 3 l_{1,1}^{(FB)d}(\frac{1}{2}h^2\kappa, \epsilon_g; \eta_\psi, \eta_\Phi) \right. \\ &- \left. l_{1,1}^{(FB)d}(\frac{1}{2}h^2\kappa, \epsilon_g + 2\lambda\kappa; \eta_\psi, \eta_\Phi) \right\} . \end{aligned} \tag{59}$$

Similarly, the scalar and quark anomalous dimensions are infered from

$$\begin{aligned} \eta_\Phi &\equiv -\frac{d}{dt}\ln Z_{\Phi,k} = 4\frac{v_d}{d}\left\{ 4\kappa\lambda^2 m_{2,2}^d(\epsilon_g, \epsilon_g + 2\lambda\kappa; \eta_\Phi) \right. \\ &+ \left. 2^{\frac{d}{2}} N_c h^2 m_4^{(F)d}(\frac{1}{2}h^2\kappa; \eta_\psi) \right\} , \\ \eta_\psi &\equiv -\frac{d}{dt}\ln Z_{\psi,k} = 2\frac{v_d}{d}h^2 \left\{ 3 m_{1,2}^{(FB)d}(\frac{1}{2}h^2\kappa, \epsilon_g; \eta_\psi, \eta_\Phi) \right. \\ &+ \left. m_{1,2}^{(FB)d}(\frac{1}{2}h^2\kappa, \epsilon_g + 2\lambda\kappa; \eta_\psi, \eta_\Phi) \right\} , \end{aligned} \tag{60}$$

which is a linear set of equations for the anomalous dimensions. The definitions of the threshold functions $l_{n_1,n_2}^{(FB)d}$, m_{n_1,n_2}^d, $m_4^{(F)d}$ and $m_{n_1,n_2}^{(FB)d}$ are again specified in[47].

The flow equations (55), (58)—(60), constitute a coupled system of ordinary and partial differential equations which can be integrated numerically[53, 54]. Here we take the effective current quark mass dependence of h, $Z_{\Phi,k}$ and $Z_{\psi,k}$ into account by stopping the evolution according to Eqs.(59), (60), evaluated for the chiral limit, below the pion mass m_π.

Similarly to the case of the quartic truncation of the effective average potential described in the preceding section one finds for $d = 4$ that chiral symmetry breaking indeed occurs for a wide range of initial values of the parameters. These include the presumably realistic case of large renormalized Yukawa coupling and a bare mass $\overline{m}_{k_\Phi}$ of order 100 MeV.

Most importantly, the approximate partial IR fixed point behavior encountered for the quartic potential approximation before, carries over to the truncation of Γ_k which maintains the full effective average potential[52]. To see this explicitly we study the flow equations (55), (58)—(60) subject to the condition $Z_{\Phi,k_\Phi} \ll 1$. For the relevant range of $\tilde{\rho}$ both $u'(t,\tilde{\rho})$ and $u'(t,\tilde{\rho}) + 2\tilde{\rho}u''(t,\tilde{\rho})$ are then much larger than $\tilde{\rho}h^2(t)$ and we may therefore neglect in the flow equations all scalar contributions with threshold functions involving these large masses. This yields the simplified equations ($d = 4$, $v_4^{-1} = 32\pi^2$)

$$\begin{aligned} \frac{\partial}{\partial t}u &= -4u + (2 + \eta_\Phi)\,\tilde{\rho}u' - \frac{N_c}{2\pi^2} l_0^{(F)4}(\frac{1}{2}\tilde{\rho}h^2) , \\ \frac{d}{dt}h^2 &= \frac{N_c}{8\pi^2}h^4 , \\ \eta_\Phi &= \frac{N_c}{8\pi^2}h^2 , \quad \eta_\psi = 0 . \end{aligned} \tag{61}$$

Again, this approximation is only valid for the initial range of running below k_Φ before the (dimensionless) renormalized scalar mass squared $u'(t,\tilde\rho=0)$ approaches zero near the chiral symmetry breaking scale. The system Eq.(61) is exactly soluble. We find

$$\begin{aligned} h^2(t) &= Z_\Phi^{-1}(t) = \frac{h_I^2}{1-\frac{N_c}{8\pi^2}h_I^2 t}\ , \quad Z_\psi(t)=1\ , \\ u(t,\tilde\rho) &= e^{-4t}u_I(e^{2t}\tilde\rho\frac{h^2(t)}{h_I^2}) - \frac{N_c}{2\pi^2}\int_0^t dr e^{-4r} l_0^{(F)4}(\frac{1}{2}h^2(t)\tilde\rho e^{2r})\ . \end{aligned} \tag{62}$$

(The integration over r on the right hand side of the solution for u can be carried out by first exchanging it with the one over momentum implicit in the definition of the threshold function $l_0^{(F)4}$.) Here $u_I(\tilde\rho)\equiv u(0,\tilde\rho)$ denotes the effective average potential at the compositeness scale and h_I^2 is the initial value of h^2 at k_Φ, i.e. for $t=0$. For simplicity we will use an expansion of the initial value effective potential $u_I(\tilde\rho)$ in powers of $\tilde\rho$ around $\tilde\rho=0$

$$u_I(\tilde\rho) = \sum_{n=0}^{\infty}\frac{u_I^{(n)}(0)}{n!}\tilde\rho^n \tag{63}$$

even though this is not essential for the forthcoming reasoning. Expanding also $l_0^{(F)4}$ in Eq.(62) in powers of its argument one finds for $n>2$

$$\frac{u^{(n)}(t,0)}{h^{2n}(t)} = e^{2(n-2)t}\frac{u_I^{(n)}(0)}{h_I^{2n}} + \frac{N_c}{\pi^2}\frac{(-1)^n(n-1)!}{2^{n+2}(n-2)} l_n^{(F)4}(0)\left[1-e^{2(n-2)t}\right]\ . \tag{64}$$

For decreasing $t\to-\infty$ the initial values $u_I^{(n)}$ become rapidly unimportant and $u^{(n)}/h^{2n}$ approaches a fixed point. For $n=2$, i.e., for the quartic coupling, one finds

$$\frac{u^{(2)}(t,0)}{h^2(t)} = 1 - \frac{1-\frac{u_I^{(2)}(0)}{h_I^2}}{1-\frac{N_c}{8\pi^2}h_I^2 t} \tag{65}$$

leading to the fixed point value $(u^{(2)}/h^2)_* = 1$ already encountered in Eq.(49). As a consequence of this fixed point behavior the system looses all its "memory" on the initial values $u_I^{(n\geq 2)}$ at the compositeness scale k_Φ! This typically happens before the approximation $u'(t,\tilde\rho), u'(t,\tilde\rho)+2\tilde\rho u''(t,\tilde\rho)\gg\tilde\rho h^2(t)$ breaks down and the solution Eq.(62) becomes invalid. Furthermore, the attraction to partial infrared fixed points continues also for the range of k where the scalar fluctuations cannot be neglected anymore. As for the quartic truncation the initial value for the bare dimensionless mass parameter

$$\frac{u_I'(0)}{h_I^2} = \frac{\overline{m}_{k_\Phi}^2}{k_\Phi^2} \tag{66}$$

is never negligible. (In fact, using the values for $\overline{m}_{k_\Phi}^2$ and k_Φ computed previously[33] for a pure quark effective action as described above one obtains $\overline{m}_{k_\Phi}^2/k_\Phi^2\simeq 0.036$.) For large h_I (and dropping the constant piece $u_I(0)$) the solution Eq.(62) therefore behaves with growing $|t|$ as

$$\begin{aligned} Z_\Phi(t) &\simeq -\frac{N_c}{8\pi^2}t\ , \quad Z_\psi(t)=1\ , \\ h^2(t) &\simeq -\frac{8\pi^2}{N_c t}\ , \\ u(t,\tilde\rho) &\simeq \frac{u_I'(0)}{h_I^2}e^{-2t}h^2(t)\tilde\rho - \frac{N_c}{2\pi^2}\int_0^t dr e^{-4r} l_0^{(F)4}(\frac{1}{2}h^2(t)\tilde\rho e^{2r})\ . \end{aligned} \tag{67}$$

Table 1. The table shows the dependence on the constituent quark mass M_q of the input parameters k_Φ, $\overline{m}^2_{k_\Phi}/k_\Phi^2$ and $\jmath$ as well as some of our "predictions". The phenomenological input used here besides M_q is $f_\pi = 92.4\,\mathrm{MeV}$, $m_\pi = 135\,\mathrm{MeV}$.The first line corresponds to the values for M_q and λ_I used in the remainder of this work. The other three lines demonstrate the insensitivity of our results with respect to the precise values of these parameters.

$\frac{M_q}{\mathrm{MeV}}$	$\frac{\lambda_I}{h_I^2}$	$\frac{k_\Phi}{\mathrm{MeV}}$	$\frac{\overline{m}^2_{k_\Phi}}{k_\Phi^2}$	$\frac{\jmath^{1/3}}{\mathrm{MeV}}$	$\frac{\hat{m}(k_\Phi)}{\mathrm{MeV}}$	$\frac{\hat{m}(1\,\mathrm{GeV})}{\mathrm{MeV}}$	$\frac{\langle\overline{\psi}\psi\rangle(1\,\mathrm{GeV})}{\mathrm{MeV}^3}$	$\frac{f_\pi^{(0)}}{\mathrm{MeV}}$
303	1	618	0.0265	66.8	14.7	11.4	$-(186)^3$	80.8
300	0	602	0.026	66.8	15.8	12.0	$-(183)^3$	80.2
310	0	585	0.025	66.1	16.9	12.5	$-(180)^3$	80.5
339	0	552	0.0225	64.4	19.5	13.7	$-(174)^3$	81.4

In other words, for $h_I \to \infty$ the IR behavior of the linear quark meson model will depend (in addition to the value of the compositeness scale k_Φ and the quark mass $\hat{m}$) only on one parameter, $\overline{m}^2_{k_\Phi}$. We have numerically verified this feature by starting with different values for $u_I^{(2)}(0)$. Indeed, the differences in the physical observables were found to be small. This IR stability of the flow equations leads to a perhaps surprising degree of predictive power: Not only the scalar wave function renormalization but even the full effective potential $U(\rho) = \lim_{k\to 0} U_k(\rho)$ is (approximately) fixed for $Z_{\Phi,k_\Phi} \ll 1$ once $\overline{m}_{k_\Phi}$ is known! For definiteness we will perform our numerical analysis of the full system of flow equations (55), (58)—(60) with the idealized initial value $u_I(\tilde{\rho}) = u_I'(0)\tilde{\rho}$ in the limit $h_I^2 \to \infty$. It should be stressed, though, that deviations from this idealization will lead only to small numerical deviations in the IR behavior of the linear quark meson model as long as the condition $Z_{\Phi,k_\Phi} \ll 1$ holds, say for[42] $h_I \gtrsim 15$.

With this knowledge at hand we may now fix the remaining three parameters of our model, k_Φ, $\overline{m}^2_{k_\Phi}$ and $\hat{m}$ by using $f_\pi = 92.4\,\mathrm{MeV}$, the pion mass $M_\pi = 135\,\mathrm{MeV}$ and the constituent quark mass M_q as phenomenological input. This approach differs from that of the preceding sections where we took an earlier determination of k_Φ as input for the computation of f_π. It will be better suited for precision estimates of the high temperature behavior in the following sections. Because of the uncertainty regarding the precise value of M_q we give in tab. 1 the results for several values of M_q. The first line of tab. 1 corresponds to the choice of M_q and $\lambda_I \equiv u_I''(\kappa)$ which we will use for the forthcoming analysis of the model at finite temperature. As argued analytically above the dependence on the value of λ_I is weak for large enough h_I as demonstrated numerically by the second line. Moreover, we notice that our results, and in particular the value of $\jmath$, are rather insensitive with respect to the precise value of M_q. It is remarkable that the values for k_Φ and $\overline{m}_{k_\Phi}$ are not very different from those computed[33] from four–quark interactions as described above. As compared to the analysis of the preceding sections the present truncation of Γ_k is of a higher level of accuracy: We now consider an arbitrary form of the effective average potential instead of a polynomial approximation and we have included the pieces in the threshold functions which are proportional to the anomalous dimensions. It is encouraging that the results are rather robust with respect to these improvements.

Once the parameters k_Φ, $\overline{m}^2_{k_\Phi}$ and $\hat{m}$ are fixed there are a number of "predictions" of the linear meson model which can be compared with the results obtained by other methods or direct experimental observation. First of all one may compute the value of $\hat{m}$ at a scale of $1\,\mathrm{GeV}$ which is suitable for comparison with results obtained from chiral perturbation theory[55] and sum rules[51]. For this purpose one has to account for the running of this quantity with the normalization scale from k_Φ as given in tab. 1

to the commonly used value of 1 GeV: $\hat{m}(1\,\mathrm{GeV}) = A^{-1}\hat{m}(k_\Phi)$. A reasonable estimate of the factor A is obtained from the three loop running of $\hat{m}$ in the $\overline{MS}$ scheme[51]. For $M_q \simeq 300\,\mathrm{MeV}$ corresponding to the first two lines in tab. 1 its value is $A \simeq 1.3$. The results for $\hat{m}(1\,\mathrm{GeV})$ are in acceptable agreement with recent results from other methods[55, 51] even though they tend to be somewhat larger. Closely related to this is the value of the chiral condensate

$$\left\langle \overline{\psi}\psi \right\rangle (1\,\mathrm{GeV}) \equiv -A\overline{m}^2_{k_\Phi}\left[f_\pi Z^{-1/2}_{\Phi,k=0} - 2\hat{m}\right] . \tag{68}$$

These results are quite non–trivial since not only f_π and $\overline{m}^2_{k_\Phi}$ enter but also the computed IR value $Z_{\Phi,k=0}$. We emphasize in this context that there may be substantial corrections both in the extrapolation from k_Φ to 1 GeV and because of the neglected influence of the strange quark which may be important near k_Φ. These uncertainties have only little effect on the physics at lower scales as relevant for our analysis of the temperature effects. Only the value of $\jmath$ which is fixed by m_π enters here.

A further more qualitative test concerns the mass of the sigma resonance or radial mode in the limit $k \to 0$ whose renormalized mass squared is given by

$$m^2_\sigma = Z^{-1/2}_{\Phi,k_\Phi}\frac{\overline{m}^2_{k_\Phi}\hat{m}}{\sigma_0} + 4\lambda\sigma_0^2 . \tag{69}$$

From our numerical analysis we obtain $\lambda_{k=0} \simeq 20$ which translates into $m_\sigma \simeq 430\,\mathrm{MeV}$. One should note, though, that this result is presumably not very accurate as we have employed in this work the approximation of using the Goldstone boson wave function renormalization constant also for the radial mode. Furthermore, the explicit chiral symmetry breaking contribution to m^2_σ is certainly underestimated as long as the strange quark is neglected. In any case, we observe that the sigma meson is significantly heavier than the pions. This is a crucial consistency check for the linear quark meson model. A low sigma mass would be in conflict with the numerous successes of chiral perturbation theory[36] which requires the decoupling of all modes other than the Goldstone bosons in the IR–limit of QCD. The decoupling of the sigma meson is, of course, equivalent to the limit $\lambda \to \infty$ which formally describes the transition from the linear to the non–linear sigma model and which appears to be reasonably well realized by the large IR–values of λ obtained in our analysis. We also note that the issue of the sigma mass is closely connected to the value of $f_\pi^{(0)}$, the value of f_π in the chiral limit $\hat{m} = 0$ also given in tab. 1. To lowest order in $(f_\pi - f_\pi^{(0)})/f_\pi$ or, equivalently, in $\hat{m}$ one has

$$f_\pi - f_\pi^{(0)} = \frac{\jmath}{Z_\Phi^{1/2} m^2_\sigma} = \frac{f_\pi m^2_\pi}{m^2_\sigma} . \tag{70}$$

A larger value of m_σ would therefore reduce the difference between $f_\pi^{(0)}$ and f_π.

In fig. 4 we show the dependence of the pion mass and decay constant on the average current quark mass $\hat{m}$. These curves depend very little on the values of the initial parameters as demonstrated in tab. 1 by $f_\pi^{(0)}$. We observe a relatively large difference of 12 MeV between the pion decay constants at $\hat{m} = \hat{m}_{\mathrm{phys}}$ and $\hat{m} = 0$. According to Eq.(70) this difference is related to the mass of the sigma particle and will be modified in the three flavor case. We will later find that the critical temperature T_c for the second order phase transition in the chiral limit is almost independent of the initial conditions. The values of $f_\pi^{(0)}$ and T_c essentially determine the non–universal amplitudes in the critical scaling region (see below). In summary, we find that the behavior of our model for small k is quite robust as far as uncertainties in the initial conditions at the scale k_Φ are concerned. We will see that the difference of observables between non–vanishing and vanishing temperature is entirely determined by the flow of couplings in the range $0 < k \lesssim 3T$.

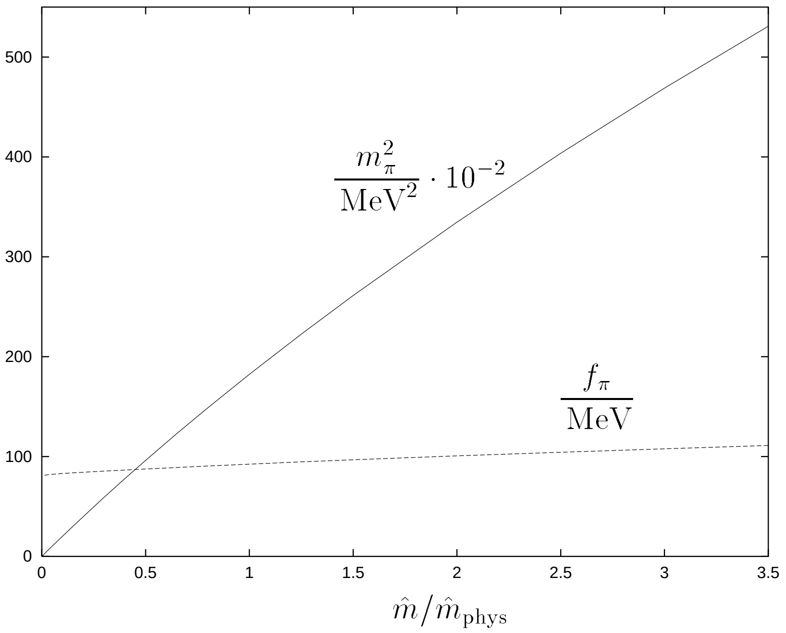

Figure 4. The plot shows m_π^2 (solid line) and f_π (dashed line) as functions of the current quark mass $\hat{m}$ in units of the physical value $\hat{m}_{\mathrm{phys}}$.

CHIRAL PHASE TRANSITION OF TWO FLAVOR QCD

Strong interactions in thermal equilibrium at high temperature T — as realized in early stages of the evolution of the Universe — differ in important aspects from the well tested vacuum or zero temperature properties. A phase transition at some critical temperature T_c or a relatively sharp crossover may separate the high and low temperature physics[56]. Many experimental activities at heavy ion colliders[57] search for signs of such a transition. It was realized early that the transition should be closely related to a qualitative change in the chiral condensate according to the general observation that spontaneous symmetry breaking tends to be absent in a high temperature situation. A series of stimulating contributions[58, 59, 60] pointed out that for sufficiently small up and down quark masses, m_u and m_d, and for a sufficiently large mass of the strange quark, m_s, the chiral transition is expected to belong to the universality class of the $O(4)$ Heisenberg model. This means that near the critical temperature only the pions and the sigma particle play a role for the behavior of condensates and long distance correlation functions. It was suggested[59, 60] that a large correlation length may be responsible for important fluctuations or lead to a disoriented chiral condensate[61]. This was even related[59, 60] to the spectacular "Centauro events"[62] observed in cosmic rays. The question how small m_u and m_d would have to be in order to see a large correlation length near T_c and if this scenario could be realized for realistic values of the current quark masses remained, however, unanswered. The reason was the missing link between the universal behavior near T_c and zero current quark mass on one hand and the known physical properties at $T = 0$ for realistic quark masses on the other hand.

It is the purpose of the remaining sections of these lectures to provide this link[52]. We present here the equation of state for two flavor QCD within an effective quark meson model. The equation of state expresses the chiral condensate $\left\langle \overline{\psi}\psi \right\rangle$ as a function of temperature and the average current quark mass $\hat{m} = (m_u + m_d)/2$. This connects explicitly the universal critical behavior for $T \to T_c$ and $\hat{m} \to 0$ with the temperature dependence for a realistic value $\hat{m}_{\rm phys}$. Since our discussion covers the whole temperature range $0 \leq T \lesssim 1.7\,T_c$ we can fix $\hat{m}_{\rm phys}$ such that the (zero temperature) pion mass is $m_\pi = 135\,{\rm MeV}$. The condensate $\left\langle\overline{\psi}\psi\right\rangle$ plays here the role of an order parameter. Fig. 5 shows our results for $\left\langle\overline{\psi}\psi\right\rangle(T,\hat{m})$: Curve (a) gives the temperature dependence of $\left\langle\overline{\psi}\psi\right\rangle$ in the chiral limit $\hat{m}=0$. Here the lower curve is the full result for arbitrary T whereas the upper curve corresponds to the universal scaling form of the equation of state for the $O(4)$ Heisenberg model. We see perfect agreement of both curves for T sufficiently close to $T_c = 100.7\,{\rm MeV}$. This demonstrates the capability of our method to cover the critical behavior and, in particular, to reproduce the critical exponents of the $O(4)$–model. We have determined (see below) the universal critical equation of state as well as the non–universal amplitudes. This provides the full functional dependence of $\left\langle\overline{\psi}\psi\right\rangle(T,\hat{m})$ for small $T-T_c$ and $\hat{m}$. The curves (b), (c) and (d) are for non–vanishing values of the average current quark mass $\hat{m}$. Curve (c) corresponds to $\hat{m}_{\rm phys}$ or, equivalently, $m_\pi(T=0) = 135\,{\rm MeV}$. One observes a crossover in the range $T = (1.2-1.5)T_c$. The $O(4)$ universal equation of state (upper curve) gives a reasonable approximation in this temperature range. The transition turns out to be much less dramatic than for $\hat{m}=0$. We have also plotted in curve (b) the results for comparably small quark masses $\simeq 1\,{\rm MeV}$, i.e. $\hat{m} = \hat{m}_{\rm phys}/10$, for which the $T=0$ value of m_π equals $45\,{\rm MeV}$. The crossover is considerably sharper but a substantial deviation from the chiral limit remains even for such small values of $\hat{m}$. In order to facilitate comparison with lattice simulations which are typically performed for larger values of m_π we also present results for $m_\pi(T=0) = 230\,{\rm MeV}$ in curve (d). One may define a "pseudocritical temperature" T_{pc} associated to the smooth crossover as the inflection point of $\left\langle\overline{\psi}\psi\right\rangle(T)$ as often done in lattice simulations. Our results for this definition of T_{pc} are denoted by $T_{pc}^{(1)}$ and are presented in tab. 2 for the four different values of $\hat{m}$ or, equivalently,

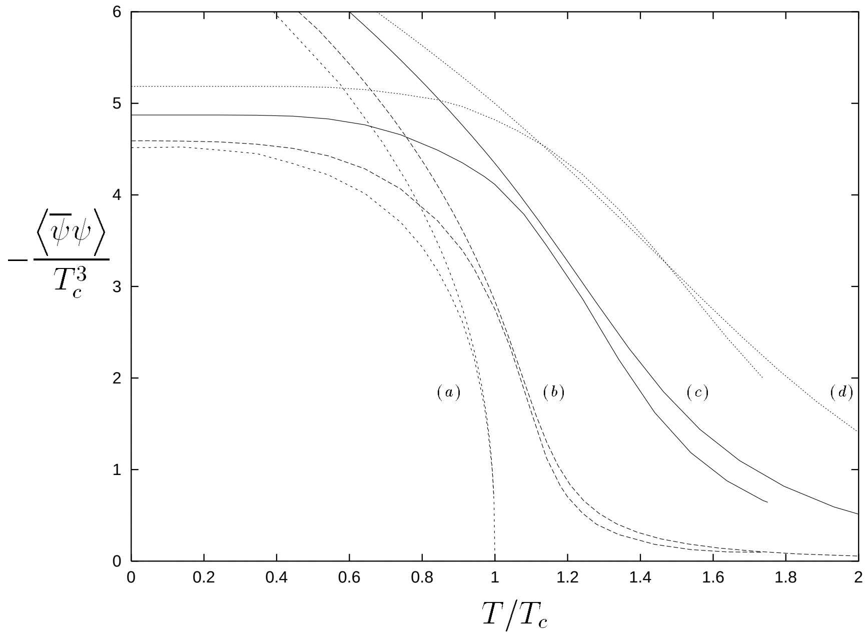

Figure 5. The plot shows the chiral condensate $\left\langle\overline{\psi}\psi\right\rangle$ as a function of temperature T. Lines (a), (b), (c), (d) correspond at zero temperature to $m_\pi = 0, 45\,{\rm MeV}, 135\,{\rm MeV}, 230\,{\rm MeV}$, respectively. For each pair of curves the lower one represents the full T–dependence of $\left\langle\overline{\psi}\psi\right\rangle$ whereas the upper one shows for comparison the universal scaling form of the equation of state for the $O(4)$ Heisenberg model. The critical temperature for zero quark mass is $T_c = 100.7\,{\rm MeV}$. The chiral condensate is normalized at a scale $k_\Phi \simeq 620\,{\rm MeV}$.

Table 2. The table shows the critical and "pseudocritical" temperatures for various values of the zero temperature pion mass. Here $T_{pc}^{(1)}$ is defined as the inflection point of $\langle\overline{\psi}\psi\rangle(T)$ whereas $T_{pc}^{(2)}$ is the location of the maximum of the sigma correlation length.

$\frac{m_\pi}{\mathrm{MeV}}$	0	45	135	230
$\frac{T_{pc}^{(1)}}{\mathrm{MeV}}$	100.7	$\simeq 110$	$\simeq 130$	$\simeq 150$
$\frac{T_{pc}^{(2)}}{\mathrm{MeV}}$	100.7	113	128	—

$m_\pi(T=0)$. The value for the pseudocritical temperature for $m_\pi = 230\,\mathrm{MeV}$ compares well with the lattice results for two flavor QCD (cf. the discussion below). One should mention, though, that a determination of T_{pc} according to this definition is subject to sizeable numerical uncertainties for large pion masses as the curve in fig. 5 is almost linear around the inflection point for quite a large temperature range. A difficult point in lattice simulations with large quark masses is the extrapolation to realistic values of m_π or even to the chiral limit. Our results may serve here as an analytic guide. The overall picture shows the approximate validity of the $O(4)$ scaling behavior over a large temperature interval in the vicinity of and above T_c once the (non–universal) amplitudes are properly computed.

A second important result of our investigations is the temperature dependence of the space–like pion correlation length $m_\pi^{-1}(T)$. (We will often call $m_\pi(T)$ the temperature dependent pion mass since it coincides with the physical pion mass for $T=0$.) The plot for $m_\pi(T)$ in fig. 6 again shows the second order phase transition in the chiral limit $\hat{m}=0$. For $T<T_c$ the pions are massless Goldstone bosons whereas for $T>T_c$ they form together with the sigma particle a degenerate vector of $O(4)$ whose mass increases as a function of temperature. For $\hat{m}=0$ the behavior for small positive $T-T_c$ is characterized by the critical exponent ν, i.e. $m_\pi(T) = (\xi^+)^{-1} T_c\,((T-T_c)/T_c)^\nu$ and we

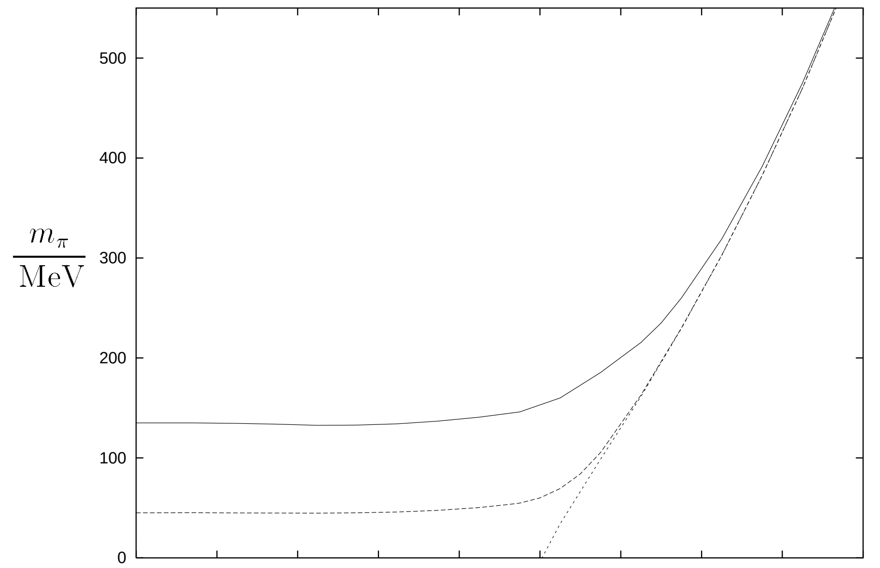

Figure 6. The plot shows m_π as a function of temperature T for three different values of the average light current quark mass $\hat{m}$. The solid line corresponds to the realistic value $\hat{m}=\hat{m}_{\mathrm{phys}}$ whereas the dotted line represents the situation without explicit chiral symmetry breaking, i.e., $\hat{m}=0$. The intermediate, dashed line assumes $\hat{m}=\hat{m}_{\mathrm{phys}}/10$.

obtain $\nu = 0.787$, $\xi^+ = 0.270$. For $\hat{m} > 0$ we find that $m_\pi(T)$ remains almost constant for $T \lesssim T_c$ with only a very slight dip for T near $T_c/2$. For $T > T_c$ the correlation length decreases rapidly and for $T \gg T_c$ the precise value of $\hat{m}$ becomes irrelevant. We see that the universal critical behavior near T_c is quite smoothly connected to $T = 0$. The full functional dependence of $m_\pi(T, \hat{m})$ allows us to compute the overall size of the pion correlation length near the critical temperature and we find $m_\pi(T_{pc}) \simeq 1.7 m_\pi(0)$ for the realistic value $\hat{m}_{\rm phys}$. This correlation length is even smaller than the vacuum ($T = 0$) one and shows no indication for strong fluctuations of pions with long wavelength. It would be interesting to see if a decrease of the pion correlation length at and above T_c is experimentally observable. It should be emphasized, however, that a tricritical behavior with a massless excitation remains possible for three flavors. This would not be characterized by the universal behavior of the $O(4)$–model. We also point out that the present investigation for the two flavor case does not take into account a speculative "effective restoration" of the axial $U_A(1)$ symmetry at high temperature[58, 63]. We will comment on these issues in the last section. In the next sections we will describe the formalism which leads to these results.

THERMAL EQUILIBRIUM AND DIMENSIONAL REDUCTION

The extension of flow equations to thermal equilibrium situations at non–vanishing temperature T is straightforward[32]. In the Euclidean formalism non–zero temperature results in (anti–)periodic boundary conditions for (fermionic) bosonic fields in the Euclidean time direction with periodicity[64] $1/T$. This leads to the replacement

$$\int \frac{d^d q}{(2\pi)^d} f(q^2) \to T \sum_{l \in \mathbb{Z}} \int \frac{d^{d-1}\vec{q}}{(2\pi)^{d-1}} f(q_0^2(l) + \vec{q}^{\,2}) \tag{71}$$

in the trace in Eq.(11) when represented as a momentum integration, with a discrete spectrum for the zero component

$$q_0(l) = \begin{cases} 2l\pi T & \text{for bosons} \\ (2l+1)\pi T & \text{for fermions}\,. \end{cases} \tag{72}$$

Hence, for $T > 0$ a four–dimensional QFT can be interpreted as a three–dimensional model with each bosonic or fermionic degree of freedom now coming in an infinite number of copies labeled by $l \in \mathbb{Z}$ (Matsubara modes). Each mode acquires an additional temperature dependent effective mass term $q_0^2(l)$. In a high temperature situation where all massive Matsubara modes decouple from the dynamics of the system one therefore expects to observe an effective three–dimensional theory with the bosonic zero modes as the only relevant degrees of freedom. In other words, if the characteristic length scale associated with the physical system is much larger than the inverse temperature the compactified Euclidean "time" dimension cannot be resolved anymore. This phenomenon is known as "dimensional reduction"[65].

The formalism of the effective average action automatically provides the tools for a smooth decoupling of the massive Matsubara modes as the scale k is lowered from $k \gg T$ to $k \ll T$. It therefore allows us to directly link the low–T, four–dimensional QFT to the effective three–dimensional high–T theory. The replacement Eq.(71) in Eq.(11) manifests itself in the flow equations (55), (58)—(60) only through a change to T–dependent threshold functions. For instance, the dimensionless functions $l_n^d(w; \eta_\Phi)$

defined in Eq.(44) are replaced by

$$l_n^d(w, \frac{T}{k}; \eta_\Phi) \equiv \frac{n+\delta_{n,0}}{4} v_d^{-1} k^{2n-d} T \sum_{l\in\mathbb{Z}} \int \frac{d^{d-1}\vec{q}}{(2\pi)^{d-1}} \left(\frac{1}{Z_{\Phi,k}} \frac{\partial R_k(q^2)}{\partial t} \right) \frac{1}{[P(q^2)+k^2 w]^{n+1}} \tag{73}$$

where $q^2 = q_0^2 + \vec{q}^{\,2}$ and $q_0 = 2\pi l T$. A list of the various temperature dependent threshold functions appearing in the flow equations can be found[52]. There we also discuss some subtleties regarding the definition of the Yukawa coupling and the anomalous dimensions for $T \neq 0$. In the limit $k \gg T$ the sum over Matsubara modes approaches the integration over a continuous range of q_0 and we recover the zero temperature threshold function $l_n^d(w;\eta_\Phi)$. In the opposite limit $k \ll T$ the massive Matsubara modes ($l \neq 0$) are suppressed and we expect to find a $d-1$ dimensional behavior of l_n^d. In fact, one obtains from Eq.(73)

$$\begin{aligned} l_n^d(w, T/k; \eta_\Phi) &\simeq l_n^d(w;\eta_\Phi) && \text{for} \quad T \ll k \,, \\ l_n^d(w, T/k; \eta_\Phi) &\simeq \frac{T}{k}\frac{v_{d-1}}{v_d} l_n^{d-1}(w;\eta_\Phi) && \text{for} \quad T \gg k \,. \end{aligned} \tag{74}$$

For our choice of the infrared cutoff function R_k, Eq.(8), the temperature dependent Matsubara modes in $l_n^d(w, T/k; \eta_\Phi)$ are exponentially suppressed for $T \ll k$ whereas the behavior is more complicated for other threshold functions appearing in the flow equations (55), (58)—(60). Nevertheless, all bosonic threshold functions are proportional to T/k for $T \gg k$ whereas those with fermionic contributions vanish in this limit¶. This behavior is demonstrated in fig. 7 where we have plotted the quotients $l_1^4(w, T/k)/l_1^4(w)$ and $l_1^{(F)4}(w, T/k)/l_1^{(F)4}(w)$ of bosonic and fermionic threshold functions, respectively. One observes that for $k \gg T$ both threshold functions essentially behave as for zero temperature. For growing T or decreasing k this changes as more and more Matsubara modes decouple until finally all massive modes are suppressed. The bosonic threshold function l_1^4 shows for $k \ll T$ the linear dependence on T/k derived in Eq.(74). In particular, for the bosonic excitations the threshold function for $w \ll 1$ can be approximated with reasonable accuracy by $l_n^4(w;\eta_\Phi)$ for $T/k < 0.25$ and by $(4T/k) l_n^3(w;\eta_\Phi)$ for $T/k > 0.25$. The fermionic threshold function $l_1^{(F)4}$ tends to zero for $k \ll T$ since there is no massless fermionic zero mode, i.e. in this limit all fermionic contributions to the flow equations are suppressed. On the other hand, the fermions remain quantitatively relevant up to $T/k \simeq 0.6$ because of the relatively long tail in fig. 7b. The transition from four to three–dimensional threshold functions leads to a *smooth dimensional reduction* as k is lowered from $k \gg T$ to $k \ll T$! Whereas for $k \gg T$ the model is most efficiently described in terms of standard four–dimensional fields Φ a choice of rescaled three–dimensional variables $\Phi_3 = \Phi/\sqrt{T}$ becomes better adapted for $k \ll T$. Accordingly, for high temperatures one will use a potential

$$u_3(t, \tilde{\rho}_3) = \frac{k}{T} u(t, \tilde{\rho}) \; ; \quad \tilde{\rho}_3 = \frac{k}{T}\tilde{\rho} \,. \tag{75}$$

In this regime $\Gamma_{k\to 0}$ corresponds to the free energy of classical statistics and $\Gamma_{k>0}$ is a classical coarse grained free energy.

For our numerical calculations at non–vanishing temperature we exploit the discussed behavior of the threshold functions by using the zero temperature flow equations in the range $k \geq 10T$. For smaller values of k we approximate the infinite Matsubara sums (cf. Eq.(73)) by a finite series such that the numerical uncertainty at $k = 10T$ is better than 10^{-4}. This approximation becomes exact in the limit $k \ll 10T$.

¶For the present choice of R_k the temperature dependence of the threshold functions is considerably smoother than in that of previous investigations[32].

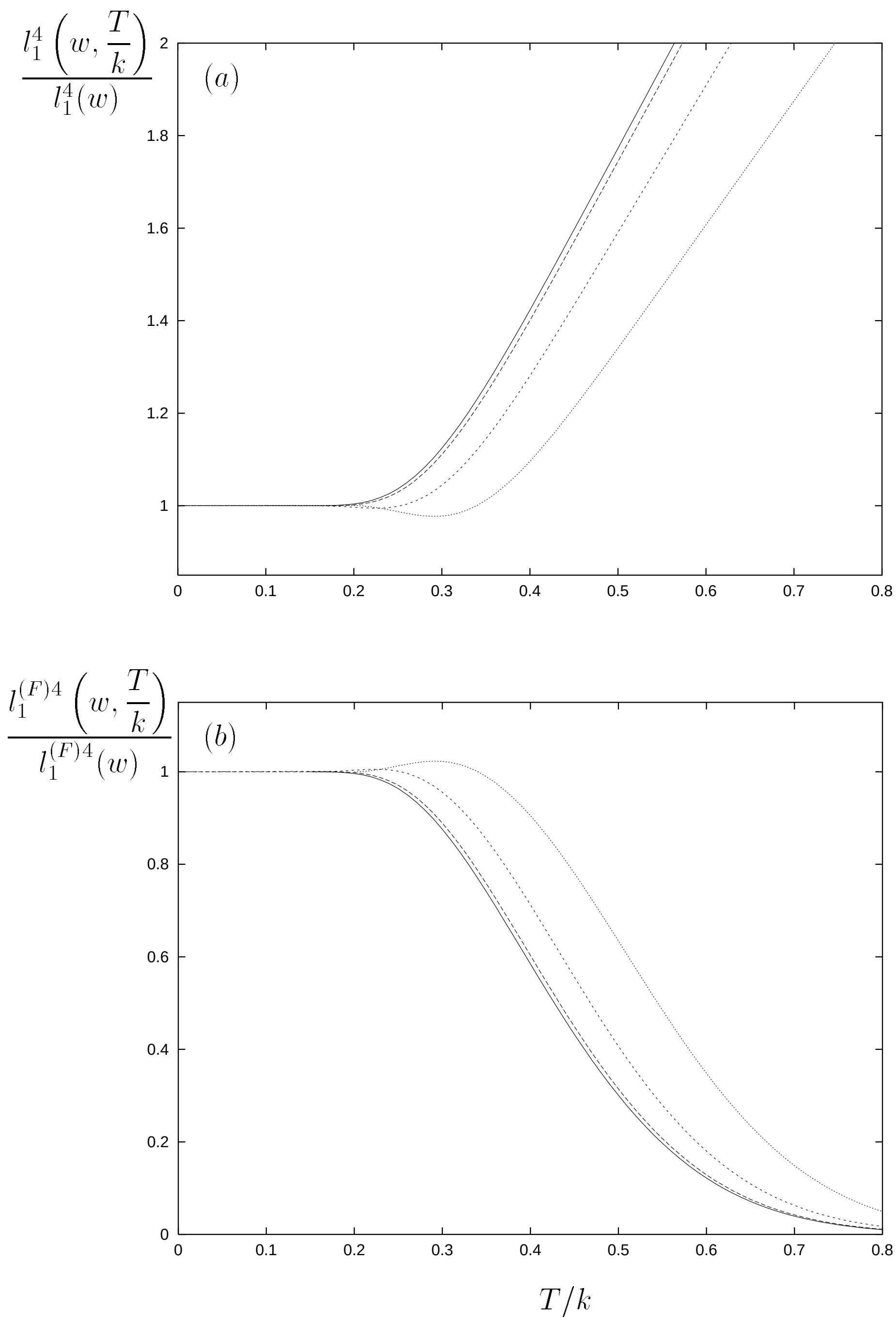

Figure 7. The plot shows the temperature dependence of the bosonic (a) and the fermionic (b) threshold functions $l_1^4(w,T/k)$ and $l_1^{(F)4}(w,T/k)$, respectively, for different values of the dimensionless mass term w. The solid line corresponds to $w=0$ whereas the dotted ones correspond to $w=0.1$, $w=1$ and $w=10$ with decreasing size of the dots. For $T \gg k$ the bosonic threshold function becomes proportional to T/k whereas the fermionic one tends to zero. In this range the theory with properly rescaled variables behaves as a classical three–dimensional theory.

THE QUARK MESON MODEL AT $T \neq 0$

So far we have considered the relevant fluctuations that contribute to the flow of Γ_k in dependence on the scale k. In a thermal equilibrium situation Γ_k also depends on the temperature T and one may ask for the relevance of thermal fluctuations at a given scale k. In particular, for not too high values of T the "initial condition" Γ_{k_Φ} for the solution of the flow equations should essentially be independent of temperature.

This will allow us to fix Γ_{k_Φ} from phenomenological input at $T = 0$ and to compute the temperature dependent quantities in the infrared ($k \to 0$). We note that the thermal fluctuations which contribute to the r.h.s. of the flow equation for the meson potential Eq.(55) are effectively suppressed for $T \lesssim k/4$ as discussed in detail in the last section. Clearly for $T \gtrsim k_\Phi/3$ temperature effects become important at the compositeness scale. We expect the linear quark meson model with a compositeness scale $k_\Phi \simeq 600\,\text{MeV}$ to be a valid description for two flavor QCD below a temperature of about $170\,\text{MeV}$. We note that there will be an effective temperature dependence of Γ_{k_Φ} induced by the fluctuations of other degrees of freedom besides the quarks, the pions and the sigma which are taken into account here. We will comment on this issue in the last section. For realistic three flavor QCD the thermal kaon fluctuations will become important for $T \gtrsim 170\,\text{MeV}$.

We compute the quantities of interest for temperatures $T \lesssim 170\,\text{MeV}$ by numerically solving the T–dependent version of the flow equations[52] (55), (58)—(60) by lowering k from k_Φ to zero. For this range of temperatures we use the initial values as given in the first line of tab. 1. This corresponds to choosing the zero temperature pion mass and the pion decay constant ($f_\pi = 92.4\,\text{MeV}$ for $m_\pi = 135\,\text{MeV}$) as phenomenological input. The only further input is the constituent quark mass M_q which we vary in the range $M_q \simeq 300 - 350\,\text{MeV}$. We observe only a minor dependence of our results on M_q for the considered range of values. In particular, the value for the critical temperature T_c of the model remains almost unaffected by this variation.

We have plotted in fig. 8 the renormalized expectation value $2\sigma_0$ of the scalar field as a function of temperature for three different values of the average light current quark mass $\hat{m}$. (We remind that $2\sigma_0(T=0) = f_\pi$.) For $\hat{m} = 0$ the order parameter σ_0 of chiral symmetry breaking continuously goes to zero for $T \to T_c = 100.7\,\text{MeV}$ characterizing the phase transition to be of second order. The universal behavior of the model for small $T - T_c$ and small $\hat{m}$ is discussed in more detail in the following section. We point out that the value of T_c corresponds to $f_\pi^{(0)} = 80.8\,\text{MeV}$, i.e. the value of the pion decay constant for $\hat{m} = 0$, which is significantly lower than $f_\pi = 92.4\,\text{MeV}$ obtained for the realistic value $\hat{m}_{\text{phys}}$. If we would fix the value of the pion decay constant to be $92.4\,\text{MeV}$

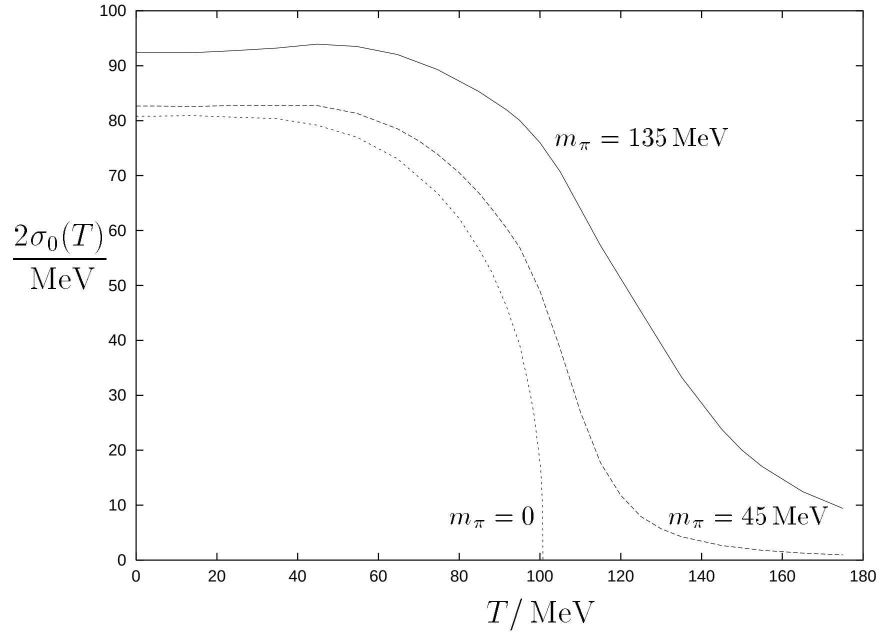

Figure 8. The expectation value $2\sigma_0$ is shown as a function of temperature T for three different values of the zero temperature pion mass.

also in the chiral limit ($\hat{m} = 0$), the value for the critical temperature would raise to 115 MeV. The nature of the transition changes qualitatively for $\hat{m} \neq 0$ where the second order transition is replaced by a smooth crossover. The crossover for a realistic $\hat{m}_{\rm phys}$ or $m_\pi(T = 0) = 135\,{\rm MeV}$ takes place in a temperature range $T \simeq (120 - 150)\,{\rm MeV}$. The middle curve in fig. 8 corresponds to a value of $\hat{m}$ which is only a tenth of the physical value, leading to a zero temperature pion mass $m_\pi = 45\,{\rm MeV}$. Here the crossover becomes considerably sharper but there remain substantial deviations from the chiral limit even for such small quark masses $\hat{m} \simeq 1\,{\rm MeV}$. The temperature dependence of m_π has already been mentioned (see fig. 6) for the same three values of $\hat{m}$. As expected, the pions behave like true Goldstone bosons for $\hat{m} = 0$, i.e. their mass vanishes for $T \leq T_c$. Interestingly, m_π remains almost constant as a function of T for $T < T_c$ before it starts to increase monotonically. We therefore find for two flavors no indication for a substantial decrease of m_π around the critical temperature.

The dependence of the mass of the sigma resonance m_σ on the temperature is displayed in fig. 9 for the above three values of $\hat{m}$. In the absence of explicit chiral symmetry breaking, $\hat{m} = 0$, the sigma mass vanishes for $T \leq T_c$. For $T < T_c$ this is a consequence of the presence of massless Goldstone bosons in the Higgs phase which drive the renormalized quartic coupling λ to zero. In fact, λ runs linearly with k for $T \gtrsim k/4$ and only evolves logarithmically for $T \lesssim k/4$. Once $\hat{m} \neq 0$ the pions acquire a mass even in the spontaneously broken phase and the evolution of λ with k is effectively stopped at $k \sim m_\pi$. Because of the temperature dependence of $\sigma_{0,k=0}$ (cf. fig. 8) this leads to a monotonically decreasing behavior of m_σ with T for $T \lesssim T_c$. This changes into the expected monotonic growth once the system reaches the symmetric phase for $T > T_c$. For low enough $\hat{m}$ one may use the minimum of $m_\sigma(T)$ for an alternative definition of the (pseudo-)critical temperature denoted as $T_{pc}^{(2)}$. Tab. 2 in the introduction shows our results for the pseudocritical temperature for different values of $\hat{m}$ or, equivalently, $m_\pi(T = 0)$. For a zero temperature pion mass $m_\pi = 135\,{\rm MeV}$ we find $T_{pc}^{(2)} = 128\,{\rm MeV}$. At larger pion masses of about 230 MeV we observe no longer a characteristic minimum for m_σ apart from a very broad, slight dip at $T \simeq 90\,{\rm MeV}$. A comparison of our results with lattice data is given below in the next section.

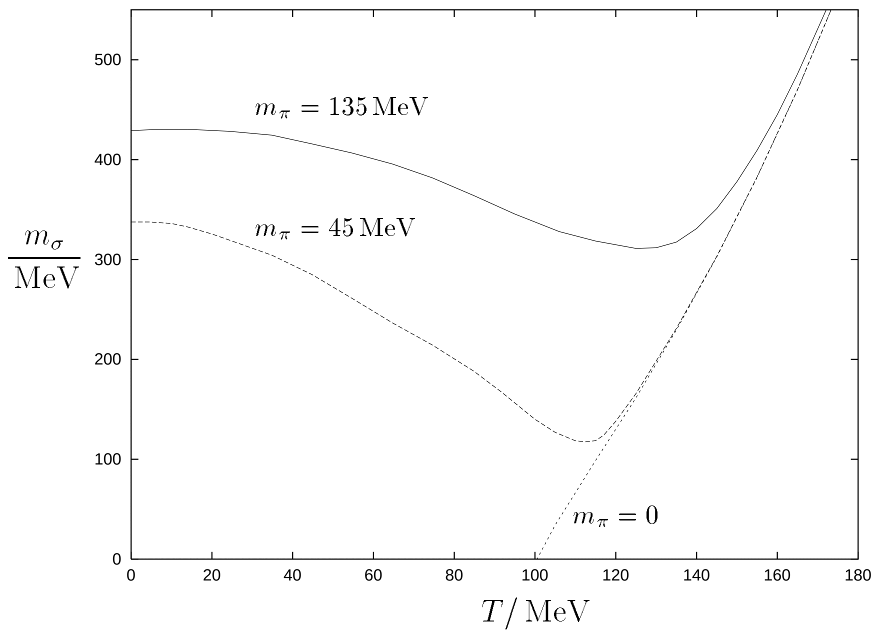

Figure 9. The plot shows the m_σ as a function of temperature T for three different values of the zero temperature pion mass.

Our results for the chiral condensate $\left\langle\overline{\psi}\psi\right\rangle$ as a function of temperature for different values of the average current quark mass are presented in fig. 5. We will compare $\left\langle\overline{\psi}\psi\right\rangle(T,\hat{m})$ with its universal scaling form for the $O(4)$ Heisenberg model in the following section.

Our ability to compute the complete temperature dependent effective meson potential U is demonstrated in fig. 10 where we display the derivative of the potential with respect to the renormalized field $\phi_R = (Z_\Phi \rho/2)^{1/2}$, for different values of T. The curves cover a temperature range $T = (5 - 175)\,\mathrm{MeV}$. The first one to the left corresponds to $T = 175\,\mathrm{MeV}$ and neighboring curves differ in temperature by $\Delta T = 10\,\mathrm{MeV}$. One observes only a weak dependence of $\partial U(T)/\partial\phi_R$ on the temperature for $T \lesssim 60\,\mathrm{MeV}$. Evaluated for $\phi_R = \sigma_0$ this function connects the renormalized field expectation value with $m_\pi(T)$, the source $\jmath$ and the mesonic wave function renormalization $Z_\Phi(T)$ according to

$$\frac{\partial U(T)}{\partial\phi_R}(\phi_R = \sigma_0) = \frac{2\jmath}{Z_\Phi^{1/2}(T)} = 4\sigma_0(T)m_\pi^2(T)\ . \tag{76}$$

We close this section with a short assessment of the validity of our effective quark meson model as an effective description of two flavor QCD at non–vanishing temperature. The identification of qualitatively different scale intervals which appear in the context of chiral symmetry breaking, as presented in the preceding sections for the zero temperature case, can be generalized to $T \neq 0$: For scales below k_Φ there exists a hybrid description in terms of quarks and mesons. For $k_{\chi SB} \leq k \lesssim 600\,\mathrm{MeV}$ chiral symmetry remains unbroken where the symmetry breaking scale $k_{\chi SB}(T)$ decreases with increasing temperature. Also the constituent quark mass decreases with T. The running Yukawa coupling depends only mildly on temperature for $T \lesssim 120\,\mathrm{MeV}$. (Only near the critical temperature and for $\hat{m} = 0$ the running is extended because of massless pion fluctuations.) On the other hand, for $k \lesssim 4T$ the effective three–dimensional gauge coupling increases faster than at $T = 0$ leading[12] to an increase of $\Lambda_{\mathrm{QCD}}(T)$ with T. As k gets closer to the scale $\Lambda_{\mathrm{QCD}}(T)$ it is no longer justified to neglect in the quark

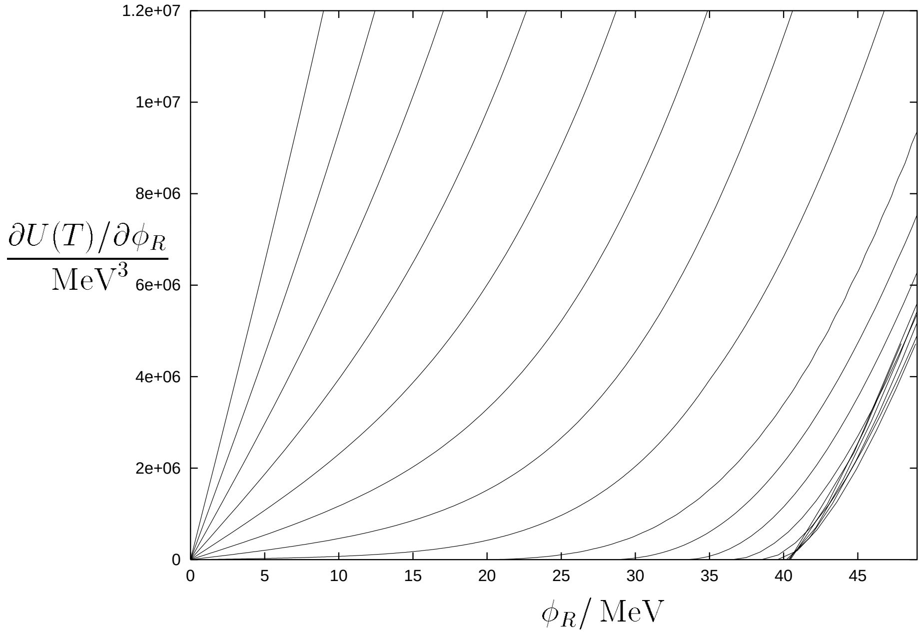

Figure 10. The plot shows the derivative of the meson potential $U(T)$ with respect to the renormalized field $\phi_R = (Z_\Phi\rho/2)^{1/2}$ for different values of T. The first curve on the left corresponds to $T = 175\,\mathrm{MeV}$. The successive curves to the right differ in temperature by $\Delta T = 10\,\mathrm{MeV}$ down to $T = 5\,\mathrm{MeV}$.

sector confinement effects which go beyond the dynamics of our present quark meson model. Here it is important to note that the quarks remain quantitatively relevant for the evolution of the meson degrees of freedom only for scales $k \gtrsim T/0.6$ (cf. fig. 7). In the limit $k \ll T/0.6$ all fermionic Matsubara modes decouple from the evolution of the meson potential according to the temperature dependent version of Eq.(55). Possible sizeable confinement corrections to the meson physics may occur if $\Lambda_{\rm QCD}(T)$ becomes larger than the maximum of $M_q(T)$ and $T/0.6$. This is particularly dangerous for small $\hat{m}$ in a temperature interval around T_c. Nevertheless, the situation is not dramatically different from the zero temperature case since only a relatively small range of k is concerned. We do not expect that the neglected QCD non–localities lead to qualitative changes. Quantitative modifications, especially for small $\hat{m}$ and $|T - T_c|$ remain possible. This would only effect the non–universal amplitudes which will be discussed in the next section. The size of these corrections depends on the strength of (non–local) deviations of the quark propagator and the Yukawa coupling from the values computed in the quark meson model.

CRITICAL BEHAVIOR NEAR THE CHIRAL PHASE TRANSITION

In this section we study the linear quark meson model in the vicinity of the critical temperature T_c close to the chiral limit $\hat{m} = 0$. In this region we find that the sigma mass m_σ^{-1} is much larger than the inverse temperature T^{-1}, and one observes an effectively three–dimensional behavior of the high temperature quantum field theory. We also note that the fermions are no longer present in the dimensionally reduced system as has been discussed above. We therefore have to deal with a purely bosonic $O(4)$–symmetric linear sigma model. At the phase transition the correlation length becomes infinite and the effective three–dimensional theory is dominated by classical statistical fluctuations. In particular, the critical exponents which describe the singular behavior of various quantities near the second order phase transition are those of the corresponding classical system.

Many properties of this system are universal, i.e. they only depend on its symmetry ($O(4)$), the dimensionality of space (three) and its degrees of freedom (four real scalar components). Universality means that the long–range properties of the system do not depend on the details of the specific model like its short distance interactions. Nevertheless, important properties as the value of the critical temperature are non–universal. We emphasize that although we have to deal with an effectively three–dimensional bosonic theory, the non–universal properties of the system crucially depend on the details of the four–dimensional theory and, in particular, on the fermions.

Our aim is a computation of the critical equation of state which relates for arbitrary T near T_c the derivative of the free energy or effective potential U to the average current quark mass $\hat{m}$. The equation of state then permits to study the temperature and quark mass dependence of properties of the chiral phase transition.

At the critical temperature and in the chiral limit there is no scale present in the theory. In the vicinity of T_c and for small enough $\hat{m}$ one therefore expects a scaling behavior of the effective average potential u_k and accordingly a universal scaling form of the equation of state[28]. There are only two independent scales close to the transition point which can be related to the deviation from the critical temperature, $T - T_c$, and to the explicit symmetry breaking through the quark mass $\hat{m}$. As a consequence, the properly rescaled potential can only depend on one scaling variable. A possible choice for the parameterization of the rescaled "unrenormalized" potential is the use of the

Table 3. The table shows the critical exponents corresponding to the three–dimensional $O(4)$–Heisenberg model. Our results are denoted by "average action" whereas "$3d$ PT" labels the exponents obtained from a $3d$ perturbative expansion using Pade techniques[70, 71]. The bottom line contains lattice Monte Carlo results.[69]

	ν	γ	δ	β	η
average action	0.787	1.548	4.80	0.407	0.0344
$3d$ PT	0.73(2)	1.44(4)	4.82(5)	0.38(1)	0.03(1)
MC	0.7479(90)	1.477(18)	4.851(22)	0.3836(46)	0.0254(38)

Widom scaling variable[66]

$$x = \frac{(T - T_c)/T_c}{(2\overline{\sigma}_0/T_c)^{1/\beta}} . \tag{77}$$

Here β is the critical exponent of the order parameter $\overline{\sigma}_0$ in the chiral limit $\hat{m} = 0$ (see Eq.(81)). With $U'(\rho = 2\overline{\sigma}_0^2) = \jmath/(2\overline{\sigma}_0)$ the Widom scaling form of the equation of state reads[66]

$$\frac{\jmath}{T_c^3} = \left(\frac{2\overline{\sigma}_0}{T_c}\right)^{\delta} f(x) \tag{78}$$

where the exponent δ is related to the behavior of the order parameter according to Eq.(83). The equation of state Eq.(78) is written for convenience directly in terms of four–dimensional quantities. They are related to the corresponding effective variables of the three–dimensional theory by appropriate powers of T_c. The source $\jmath$ is determined by the average current quark mass $\hat{m}$ as $\jmath = 2\overline{m}_{k_\Phi}^2 \hat{m}$. The mass term at the compositeness scale, $\overline{m}_{k_\Phi}^2$, also relates the chiral condensate to the order parameter according to $\left\langle \overline{\psi}\psi \right\rangle = -2\overline{m}_{k_\Phi}^2(\overline{\sigma}_0 - \hat{m})$. The critical temperature of the linear quark meson model was found above to be $T_c = 100.7\,\mathrm{MeV}$.

The scaling function f is universal up to the model specific normalization of x and itself. Accordingly, all models in the same universality class can be related by a rescaling of $\overline{\sigma}_0$ and $T - T_c$. The non–universal normalizations for the quark meson model discussed here are defined according to

$$f(0) = D \quad , \qquad f(-B^{-1/\beta}) = 0 . \tag{79}$$

We find $D = 1.82 \cdot 10^{-4}$, $B = 7.41$ and our result for β is given in tab. 3. Apart from the immediate vicinity of the zero of $f(x)$ we find the following two parameter fit for the scaling function[25],

$$\begin{aligned} f_{\rm fit}(x) &= 1.816 \cdot 10^{-4}(1 + 136.1\,x)^2\,(1 + 160.9\,\theta\,x)^{\Delta} \\ & \quad (1 + 160.9\,(0.9446\,\theta^{\Delta})^{-1/(\gamma-2-\Delta)}\,x)^{\gamma-2-\Delta} \end{aligned} \tag{80}$$

to reproduce the numerical results for f and df/dx at the $1 - 2\%$ level with $\theta = 0.625$ (0.656), $\Delta = -0.490$ (-0.550) for $x > 0$ $(x < 0)$ and γ as given in tab. 3. The universal properties of the scaling function can be compared with results obtained by other methods for the three–dimensional $O(4)$ Heisenberg model. In fig. 11 we display our results along with those obtained from lattice Monte Carlo simulation[67], second order epsilon expansion[68] and mean field theory. We observe a good agreement of average action, lattice and epsilon expansion results within a few per cent for $T < T_c$. Above T_c the average action and the lattice curve go quite close to each other with a substantial deviation from the epsilon expansion and mean field scaling function. (We note that

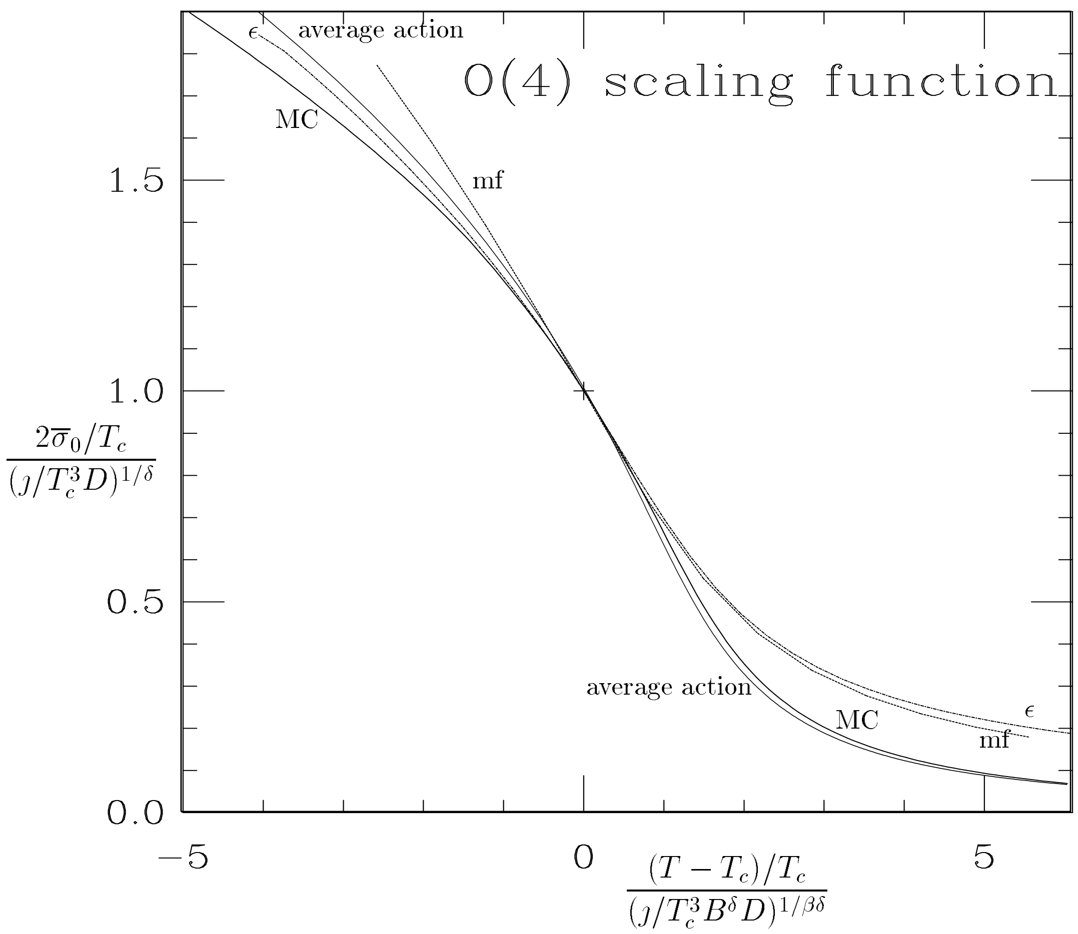

Figure 11. The figure shows a comparison of our results, denoted by "average action", with results of other methods for the scaling function of the three–dimensional $O(4)$ Heisenberg model. We have labeled the axes for convenience in terms of the expectation value $\overline{\sigma}_0$ and the source $\jmath$ of the corresponding four–dimensional theory. The constants B and D specify the non–universal amplitudes of the model (cf. Eq.(79). The curve labeled by "MC" represents a fit to lattice Monte Carlo data. The second order epsilon expansion[68] and mean field results are denoted by "ϵ" and "mf", respectively. Apart from our results the curves are taken from[67].

the question of a better agreement of the curves for $T < T_c$ or $T > T_c$ depends on the chosen non–universal normalization conditions for x and f (cf. Eq.(79)).)

Before we use the scaling function $f(x)$ to discuss the general temperature and quark mass dependent case, we consider the limits $T = T_c$ and $\hat{m} = 0$, respectively. In these limits the behavior of the various quantities is determined solely by critical amplitudes and exponents. In the spontaneously broken phase ($T < T_c$) and in the chiral limit we observe that the renormalized and unrenormalized order parameters scale according to

$$\begin{aligned}
\frac{2\sigma_0(T)}{T_c} &= (2E)^{1/2}\left(\frac{T_c - T}{T_c}\right)^{\nu/2}, \\
\frac{2\overline{\sigma}_0(T)}{T_c} &= B\left(\frac{T_c - T}{T_c}\right)^{\beta},
\end{aligned} \tag{81}$$

respectively, with $E = 0.814$ and the value of B given above. In the symmetric phase the renormalized mass $m = m_\pi = m_\sigma$ and the unrenormalized mass $\overline{m} = Z_\Phi^{1/2} m$ behave as

$$
\begin{aligned}
\frac{m(T)}{T_c} &= \left(\xi^+\right)^{-1}\left(\frac{T-T_c}{T_c}\right)^{\nu} , \\
\frac{\overline{m}(T)}{T_c} &= \left(C^+\right)^{-1/2}\left(\frac{T-T_c}{T_c}\right)^{\gamma/2} ,
\end{aligned} \tag{82}
$$

where $\xi^+ = 0.270$, $C^+ = 2.79$. For $T = T_c$ and non–vanishing current quark mass we have

$$
\frac{2\overline{\sigma}_0}{T_c} = D^{-1/\delta}\left(\frac{\jmath}{T_c^3}\right)^{1/\delta} \tag{83}
$$

with the value of D given above.

Though the five amplitudes E, B, ξ^+, C^+ and D are not universal there are ratios of amplitudes which are invariant under a rescaling of $\overline{\sigma}_0$ and $T - T_c$. Our results for the universal amplitude ratios are

$$
\begin{aligned}
R_\chi &= C^+ D B^{\delta-1} = 1.02 , \\
\tilde{R}_\xi &= (\xi^+)^{\beta/\nu} D^{1/(\delta+1)} B = 0.852 , \\
\xi^+ E &= 0.220 .
\end{aligned} \tag{84}
$$

Those for the critical exponents are given in tab. 3. Here the value of η is obtained from the temperature dependent version of Eq.(60) at the critical temperature[52]. For comparison tab. 3 also gives the results[70, 71] of a $3d$ perturbative computation as well as lattice Monte Carlo results[69] which have been used for the lattice form of the scaling function in fig. 11.[‖] There are only two independent amplitudes and critical exponents, respectively. They are related by the usual scaling relations of the three–dimensional scalar $O(N)$–model[71] which we have explicitly verified by the independent calculation of our exponents.

We turn to the discussion of the scaling behavior of the chiral condensate $\left\langle\overline{\psi}\psi\right\rangle$ for the general case of a temperature and quark mass dependence. In fig. 5 we have displayed our results for the scaling equation of state in terms of the chiral condensate

$$
\left\langle\overline{\psi}\psi\right\rangle = -\overline{m}_{k_\Phi}^2 T_c \left(\frac{\jmath/T_c^3}{f(x)}\right)^{1/\delta} + \jmath \tag{85}
$$

as a function of $T/T_c = 1 + x(\jmath/T_c^3 f(x))^{1/\beta\delta}$ for different quark masses or, equivalently, different values of $\jmath$. The curves shown in fig. 5 correspond to quark masses $\hat{m} = 0$, $\hat{m} = \hat{m}_{\rm phys}/10$, $\hat{m} = \hat{m}_{\rm phys}$ and $\hat{m} = 3.5\hat{m}_{\rm phys}$ or, equivalently, to zero temperature pion masses $m_\pi = 0$, $m_\pi = 45\,\mathrm{MeV}$, $m_\pi = 135\,\mathrm{MeV}$ and $m_\pi = 230\,\mathrm{MeV}$, respectively (cf. fig. 4). One observes that the second order phase transition with a vanishing order parameter at T_c for $\hat{m} = 0$ is turned into a smooth crossover in the presence of non–zero quark masses.

The scaling form Eq.(85) for the chiral condensate is exact only in the limit $T \to T_c$, $\jmath \to 0$. It is interesting to find the range of temperatures and quark masses for which $\left\langle\overline{\psi}\psi\right\rangle$ approximately shows the scaling behavior Eq.(85). This can be infered from a comparison (see fig. 5) with our full non–universal solution for the T and $\jmath$ dependence of $\left\langle\overline{\psi}\psi\right\rangle$. For $m_\pi = 0$ one observes approximate scaling behavior for temperatures $T \gtrsim 90\,\mathrm{MeV}$. This situation persists up to a pion mass of $m_\pi = 45\,\mathrm{MeV}$. Even for the realistic case, $m_\pi = 135\,\mathrm{MeV}$, and to a somewhat lesser extent for $m_\pi = 230\,\mathrm{MeV}$ the

‖See also ref[72] and references therein for a recent calculation of critical exponents using similar methods as in this work. For high precision estimates of the critical exponents see also refs[73, 74].

scaling curve reasonably reflects the physical behavior for $T \gtrsim T_c$. For temperatures below T_c, however, the zero temperature mass scales become important and the scaling arguments leading to universality break down.

The above comparison may help to shed some light on the use of universality arguments away from the critical temperature and the chiral limit. One observes that for temperatures above T_c the scaling assumption leads to quantitatively reasonable results even for a pion mass almost twice as large as the physical value. This in turn has been used for two flavor lattice QCD as theoretical input to guide extrapolation of results to light current quark masses. From simulations based on a range of pion masses $0.3 \lesssim m_\pi/m_\rho \lesssim 0.7$ and temperatures $0 < T \lesssim 250\,\mathrm{MeV}$ a "pseudocritical temperature" of approximately 140 MeV with a weak quark mass dependence is reported[75]. Here the "pseudocritical temperature" T_{pc} is defined as the inflection point of $\left\langle\overline{\psi}\psi\right\rangle$ as a function of temperature. The values of the lattice action parameters used in[75] with $N_t = 6$ were $a\hat{m} = 0.0125$, $6/g^2 = 5.415$ and $a\hat{m} = 0.025$, $6/g^2 = 5.445$. For comparison with lattice data we have displayed in fig. 5 the temperature dependence of the chiral condensate for a pion mass $m_\pi = 230\,\mathrm{MeV}$. From the free energy of the linear quark meson model we obtain in this case a pseudocritical temperature of about 150 MeV in reasonable agreement with the results of ref[75]. In contrast, for the critical temperature in the chiral limit we obtain $T_c = 100.7\,\mathrm{MeV}$. This value is considerably smaller than the lattice results of about $(140 - 150)\,\mathrm{MeV}$ obtained by extrapolating to zero quark mass in ref[75]. We point out that for pion masses as large as 230 MeV the condensate $\left\langle\overline{\psi}\psi\right\rangle(T)$ is almost linear around the inflection point for quite a large range of temperature. This makes a precise determination of T_c somewhat difficult. Furthermore, fig. 5 shows that the scaling form of $\left\langle\overline{\psi}\psi\right\rangle(T)$ underestimates the slope of the physical curve. Used as a fit with T_c as a parameter this can lead to an overestimate of the pseudocritical temperature in the chiral limit. We also mention here the results of ref[76]. There two values of the pseudocritical temperature, $T_{pc} = 150(9)\,\mathrm{MeV}$ and $T_{pc} = 140(8)$, corresponding to $a\hat{m} = 0.0125$, $6/g^2 = 5.54(2)$ and $a\hat{m} = 0.00625$, $6/g^2 = 5.49(2)$, respectively, (both for $N_t = 8$) were computed. These values show a somewhat stronger quark mass dependence of T_{pc} and were used for a linear extrapolation to the chiral limit yielding $T_c = 128(9)\,\mathrm{MeV}$.

The linear quark meson model exhibits a second order phase transition for two quark flavors in the chiral limit. As a consequence the model predicts a scaling behavior near the critical temperature and the chiral limit which can, in principle, be tested in lattice simulations. For the quark masses used in the present lattice studies the order and universality class of the transition in two flavor QCD remain a partially open question. Though there are results from the lattice giving support for critical scaling[77, 78] there are also recent simulations with two flavors that reveal significant finite size effects and problems with $O(4)$ scaling[79, 80].

ADDITIONAL DEGREES OF FREEDOM

So far we have investigated the chiral phase transition of QCD as described by the linear $O(4)$–model containing the three pions and the sigma resonance as well as the up and down quarks as degrees of freedom. Of course, it is clear that the spectrum of QCD is much richer than the states incorporated in our model. It is therefore important to ask to what extent the neglected degrees of freedom like the strange quark, strange (pseudo)scalar mesons, (axial)vector mesons, baryons, etc., might be important for the chiral dynamics of QCD. Before doing so it is perhaps instructive to first look into the opposite direction and investigate the difference between the linear quark meson model described here and chiral perturbation theory based on the non–linear sigma model[36]. In some sense, chiral perturbation theory is the minimal model of chiral symmetry breaking containing only the Goldstone degrees of freedom. By construction it is therefore only valid in the spontaneously broken phase and can not be expected to yield realistic results for temperatures close to T_c or for the symmetric phase. However, for small temperatures (and momentum scales) the non–linear model is expected to describe the low–energy and low–temperature limit of QCD reliably as an expansion in powers of the light quark masses. For vanishing temperature it has been demonstrated recently[42, 43, 44] that the results of chiral perturbation theory can be reproduced within the linear meson model once certain higher dimensional operators in its effective action are taken into account for the three flavor case. Moreover, some of the parameters of chiral perturbation theory ($L_4, \ldots, L_8$) can be expressed and therefore also numerically computed in terms of those of the linear model. For non–vanishing temperature one expects agreement only for low T whereas deviations from chiral perturbation theory should become large close to T_c. Yet, even for $T \ll T_c$ small quantitative deviations should exist because of the contributions of (constituent) quark and sigma meson fluctuations in the linear model which are not taken into account in chiral perturbation theory.

From[81] we infer the three–loop result for the temperature dependence of the chiral condensate in the chiral limit for N light flavors

$$\begin{aligned}
\left\langle\overline{\psi}\psi\right\rangle(T)_{\chi PT} &= \left\langle\overline{\psi}\psi\right\rangle_{\chi PT}(0)\left\{1-\frac{N^2-1}{N}\frac{T^2}{12F_0^2}-\frac{N^2-1}{2N^2}\left(\frac{T^2}{12F_0^2}\right)^2\right. \\
&+ \left. N(N^2-1)\left(\frac{T^2}{12F_0^2}\right)^3\ln\frac{T}{\Gamma_1}\right\}+\mathcal{O}(T^8)\,.
\end{aligned} \tag{86}$$

The scale Γ_1 can be determined from the D–wave isospin zero $\pi\pi$ scattering length and is given by $\Gamma_1 = (470 \pm 100)\,\mathrm{MeV}$. The constant F_0 is (in the chiral limit) identical to the pion decay constant $F_0 = f_\pi^{(0)} = 80.8\,\mathrm{MeV}$. In fig. 12 we have plotted the chiral

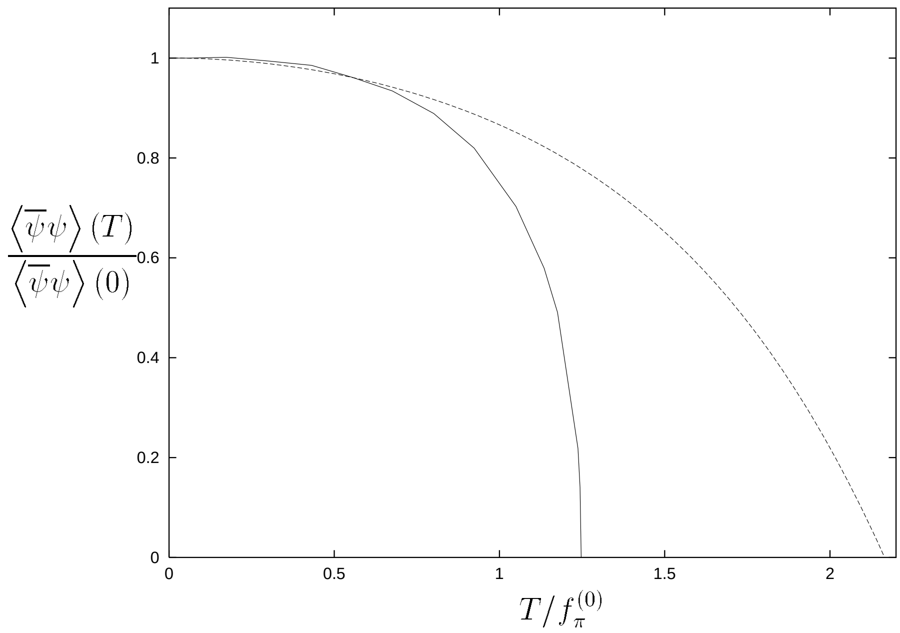

Figure 12. The plot displays the chiral condensate $\left\langle\overline{\psi}\psi\right\rangle$ as a function of $T/f_\pi^{(0)}$. The solid line corresponds to our results for vanishing average current quark mass $\hat{m} = 0$ whereas the dashed line shows the corresponding three–loop chiral perturbation theory result for $\Gamma_1 = 470\,\mathrm{MeV}$.

condensate as a function of T/F_0 for both, chiral perturbation theory according to Eq.(86) and for the linear quark meson model. As expected the agreement for small T is very good. Nevertheless, the anticipated small numerical deviations present even for $T \ll T_c$ due to quark and sigma meson loop contributions are manifest. For larger values of T, say for $T \gtrsim 0.8 f_\pi^{(0)}$ the deviations become significant because of the intrinsic inability of chiral perturbation theory to correctly reproduce the critical behavior of the system near its second order phase transition.

Within the language of chiral perturbation theory the neglected effects of thermal quark fluctuations may be described by an effective temperature dependence of the parameter $F_0(T)$. We notice that the temperature at which these corrections become important equals approximately one third of the constituent quark mass $M_q(T)$ or the sigma mass $m_\sigma(T)$, respectively, in perfect agreement with fig. 7. As suggested by this figure the onset of the effects from thermal fluctuations of heavy particles with a T–dependent mass $m_H(T)$ is rather sudden for $T \gtrsim m_H(T)/3$. These considerations also apply to our two flavor quark meson model. Within full QCD we expect temperature dependent initial values at k_Φ.

The dominant contribution to the temperature dependence of the initial values presumably arises from the influence of the mesons containing strange quarks as well as the strange quark itself. Here the quantity $\overline{m}^2_{k_\Phi}$ seems to be the most important one. (The temperature dependence of higher couplings like $\lambda(T)$ is not very relevant if the IR attractive behavior remains valid, i.e. if Z_{Φ,k_Φ} remains small for the range of temperatures considered. We neglect a possible T–dependence of the current quark mass $\hat{m}$.) In particular, for three flavors the potential U_{k_Φ} contains a term

$$-\frac{1}{2}\overline{\nu}_{k_\Phi}\left(\det\Phi + \det\Phi^\dagger\right) = -\overline{\nu}_{k_\Phi}\varphi_s\Phi_{uu}\Phi_{dd} + \dots \tag{87}$$

which reflects the axial $U_A(1)$ anomaly. It yields a contribution to the effective mass term proportional to the expectation value $\langle\Phi_{ss}\rangle \equiv \varphi_s$, i.e.

$$\Delta\overline{m}^2_{k_\Phi} = -\frac{1}{2}\overline{\nu}_{k_\Phi}\varphi_s\ . \tag{88}$$

Both, $\overline{\nu}_{k_\Phi}$ and φ_s, depend on T. We expect these corrections to become relevant only for temperatures exceeding $m_K(T)/3$ or $M_s(T)/3$. We note that the temperature dependent kaon and strange quark masses, $m_K(T)$ and $M_s(T)$, respectively, may be somewhat different from their zero temperature values but we do not expect them to be much smaller. A typical value for these scales is around 500 MeV. Correspondingly, the thermal fluctuations neglected in our model should become important for $T \gtrsim 170$ MeV. It is even conceivable that a discontinuity appears in $\varphi_s(T)$ for sufficiently high T (say $T \simeq 170$ MeV). This would be reflected by a discontinuity in the initial values of the $O(4)$–model leading to a first order transition within this model. Obviously, these questions should be addressed in the framework of the three flavor $SU_L(3) \times SU_R(3)$ quark meson model. Work in this direction is in progress.

We note that the temperature dependence of $\overline{\nu}(T)\varphi_s(T)$ is closely related to the question of an effective high temperature restoration of the axial $U_A(1)$ symmetry[58, 63]. The η' mass term is directly proportional to this combination[42], $m^2_{\eta'}(T) - m^2_\pi(T) \simeq \frac{3}{2}\overline{\nu}(T)\varphi_s(T)$. Approximate $U_A(1)$ restoration would occur if $\varphi_s(T)$ or $\overline{\nu}(T)$ would decrease sizeably for large T. For realistic QCD this question should be addressed by a three flavor study. Within two flavor QCD the combination $\overline{\nu}_k\varphi_s$ is replaced by an effective anomalous mass term $\overline{\nu}_k^{(2)}$. The temperature dependence of $\overline{\nu}^{(2)}(T)$ could be studied by introducing quarks and the axial anomaly in the two flavor matrix model of ref[54]. We add that this question has also been studied within full two flavor QCD in lattice simulations[79, 82, 83]. So far there does not seem to be much evidence for a restoration of the $U_A(1)$ symmetry near T_c but no final conclusion can be drawn yet.

To summarize, we have found that the effective two flavor quark meson model presumably gives a good description of the temperature effects in two flavor QCD for a temperature range $T \lesssim 170\,\mathrm{MeV}$. Its reliability should be best for low temperature where our results agree with chiral perturbation theory. However, the range of validity is considerably extended as compared to chiral perturbation theory and includes, in particular, the critical temperature of the second order phase transition in the chiral limit. We have explicitly connected the universal critical behavior for small $|T - T_c|$ and small current quark masses with the renormalized couplings at $T = 0$ and realistic quark masses. The main quantitative uncertainties from neglected fluctuations presumably concern the values of $f_\pi^{(0)}$ and T_c which, in turn, influence the non–universal amplitudes B and D in the critical region. We believe that our overall picture is rather solid. Where applicable our results compare well with numerical simulations of full two flavor QCD.

CONCLUSIONS

Our conclusions may be summarized in the following points:

1. The connection between short distance perturbative QCD and long distance meson physics by analytical methods seems to emerge step by step. The essential ingredients are nonperturbative flow equations as approximations of exact renormalization group equations and a formalism which allows a change of variables by introducing meson–like composite fields.

2. The relevance of meson–like $\overline{\psi}\psi$ composite objects is established in this framework. A typical scale where the mesonic bound states appear is the compositeness scale $k_\Phi \simeq (600-700)\,\mathrm{MeV}$. The occurrence of chiral symmetry breaking depends on the effective meson mass $\overline{m}_{k_\Phi}$ at the compositeness scale. For a certain range of values of the ratio $\overline{m}^2_{k_\Phi}/k^2_\Phi$ spontaneous chiral symmetry breaking is induced by quark fluctuations. A definite analytical establishment of spontaneous chiral symmetry breaking from "first principles" (i.e., short distance QCD) still awaits a reliable calculation of this ratio.

3. Phenomenologically, the ratio $\overline{m}^2_{k_\Phi}/k^2_\Phi$ may be determined from the value of the constituent quark mass in units of the pion decay constant f_π. For this value the ratios f_π/k_Φ and $\left\langle\overline{\psi}\psi\right\rangle/k^3_\Phi$ can be computed. Together with an earlier estimate of k_Φ this yields rather encouraging results: $f_\pi \simeq 100\,\mathrm{MeV}$ and $\left\langle\overline{\psi}\psi\right\rangle \simeq -(190\,\mathrm{MeV})^3$ for two flavor QCD. It will be very interesting to generalize these results to the realistic three flavor case.

4. The formalism presented here naturally leads to an effective linear quark meson model for the description of mesons below the compositeness scale k_Φ. For this model the standard non–linear sigma model of chiral perturbation theory emerges as a low energy approximation due to the large sigma mass.

5. The old puzzle about the precise connection between the current and the constituent quark mass reveals new interesting aspects in this formalism. In the context of the effective average action one may define these masses by the quark propagator at zero or very small momentum, either in the quark gluon picture (current quark mass) or the effective quark meson model (constituent quark mass). There

is no conceptual difference between the two situations. As a function of k the running quark mass smoothly interpolates between the standard current quark mass m_q for high k and the standard constituent quark mass M_q for low k. (This holds at least as long as the minimum of the effective scalar potential is unique.) A rapid quantitative change occurs for $k \simeq (400-500)$ MeV because of the onset of chiral symmetry breaking. For $k=0$ one expects this behavior to carry over to the momentum dependence of the quark propagator: For small q^2 the inverse quark propagator is dominated by M_q. In contrast, for high q^2 the constant term in the inverse propagator is reduced to m_q since q^2 replaces k^2 as an effective infrared cutoff. One expects a smooth interpolation between the two limits and it would be interesting to know the form of the propagator for momenta in the transition region. Furthermore, the symmetry breaking source term which determines the pion mass in the linear or non–linear meson model can be related to the current quark mass at the compositeness scale. This constitutes a bridge between the low energy meson properties and the running quark mass at a scale which is not too far from the validity of perturbation theory.

6. A particular version of the Nambu–Jona-Lasinio model appears in our formalism as a limiting case (infinitely strong renormalized Yukawa coupling at the compositeness scale k_Φ). Here the ultraviolet cutoff which is implicit in the NJL model is dictated by the momentum dependence of the infrared cutoff function R_k in the effective average action. The characteristic cutoff scale is k_Φ. In this context our results can be interpreted as an approximative solution of the NJL model. Our method includes many contributions beyond the leading order contribution of the $1/N_c$ expansion.

7. Based on a satisfactory understanding of the meson properties in the vacuum we have described their behavior in a thermal equilibrium situation. Our method should remain valid for temperature below ~ 170 MeV. This extends well beyond the validity of chiral perturbation theory. In particular, in the chiral limit of vanishing quark masses we can describe the universal critical behavior near a second order phase transition of two flavor QCD. The universal behavior is quantitatively connected to observed quantities at zero temperature and realistic quark masses.

Acknowledgements

We thank J. Berges and B. Bergerhoff for collaboration on many subjects covered by these lectures. We also wish to express our gratitude to the organizers of the *NATO Advanced Study Institute: Confinement, Duality and Non–perturbative Aspects of QCD* for their excellent organization and for providing a most stimulating environment.

REFERENCES

1. L.P. Kadanoff, *Physica* 2 (1966) 263.
2. K. G. Wilson, Phys. Rev. **B4** (1971) 3174; K. G. Wilson and I. G. Kogut, Phys. Rep. **12** (1974) 75.
3. F. Wegner and A. Houghton, Phys. Rev. **A8** (1973) 401; F.J. Wegner in *Phase Transitions and Critical Phenomena*, vol. 6, eds. C. Domb and M.S. Greene, Academic Press (1976); J.F. Nicoll and T.S. Chang, Phys. Lett. **62A** (1977) 287.
4. S. Weinberg in *Critical Phenomena for Field Theorists*, Erice Subnucl. Phys. (1976) 1.
5. J. Polchinski, Nucl. Phys. **B231** (1984) 269.
6. A. Hasenfratz and P. Hasenfratz, Nucl. Phys. **B270** (1986) 685; P. Hasenfratz and J. Nager, Z. Phys. **C37** (1988) 477.

7. C. Wetterich, Nucl. Phys. **B352** (1991) 529; Z. Phys. **C57** (1993) 451; C60 (1993) 461.
8. J. Schwinger, Proc. Nat. Acad. Sc. **37** (1951) 452; J. Goldstone, A. Salam and S. Weinberg, Phys. Rev. **127** (1962) 965; G. Jona–Lasinio, Nuovo Cim. **34** (1964) 1790; K. Symanzik, Comm. Math. Phys. **16** (1970) 48; J. Iliopoulos, C. Itzykson and A. Martin, Rev. Mod. Phys. **47** (1975) 165.
9. A. Ringwald and C. Wetterich, Nucl. Phys. **B334** (1990) 506; N. Tetradis and C. Wetterich, Nucl. Phys. **B383** (1992) 197.
10. C. Wetterich, Z. Phys. **C48** (1990) 693; S. Bornholdt and C. Wetterich, Z. Phys. **C58** (1993) 585.
11. J. Comelas, Y. Kubyshin and E.Moreno, Nucl. Phys. **B490** (1997) 653 (hep-th/9512086).
12. M. Reuter and C. Wetterich, Nucl. Phys. **B391** (1993) 147; B408 (1993) 91; B417 (1994) 181; B427 (1994) 291; preprint HD-THEP-94-39 (hep-th/9708051).
13. C. Becchi, Lecture given at the Parma Theoretical Physics Seminar, Sep 1991, preprint GEF-TH-96-11 (hep-th/9607188).
14. M. Bonini, M. D'Attanasio, and G. Marchesini, Nucl. Phys. **B418** (1994) 81; B421 (1994) 429.
15. U. Ellwanger, Phys. Lett. **B335** (1994) 364; U. Ellwanger, M. Hirsch and A. Weber, Z. Phys. **C69** (1996) 687.
16. C. Wetterich, preprint HD–THEP–95–2 (hep-th/9501119); Z. Phys. **C72** (1996) 139 (hep-ph/9604227).
17. U. Ellwanger, M. Hirsch and A. Weber, preprint LPTHE Orsay 96–50 (hep-ph/9606468).
18. B. Bergerhoff and C. Wetterich, preprint HD–THEP–97–46 (hep-ph/9708425).
19. G. Keller, C. Kopper and M. Salmhofer, Helv. Phys. Acta **65** (1992) 32; G. Keller and G. Kopper, Phys. Lett. **273B** (1991) 323.
20. C. Wetterich, Phys. Lett. **301B** (1993) 90.
21. C. Wetterich, Mod. Phys. Lett. **A11** (1996) 2573 (hep-th/9602039).
22. M. Bonini, M. D'Attanasio, and G. Marchesini, Nucl. Phys. **B409** (1993) 441; U. Ellwanger, Z. Phys. **C58** (1993) 619; C. Wetterich, Int. J. Mod. Phys. **A9** (1994) 3571.
23. F.J. Dyson, Phys. Rev. **75** (1949) 1736; J. Schwinger, Proc. Nat. Acad. Sc. **37** (1951) 452.
24. J. Adams, J. Berges, S. Bornholdt, F. Freire, N. Tetradis and C. Wetterich, Mod. Phys. Lett. **A10** (1995) 2367.
25. J. Berges, N. Tetradis and C. Wetterich, Phys. Rev. Lett. **77** (1996) 873.
26. N. Tetradis, Nucl. Phys. **B488** (1997) 92 (hep-ph/9608272)
27. J. Berges and C. Wetterich, Nucl. Phys. **B487** (1997) 675 (hep-th/9609019).
28. N. Tetradis and C. Wetterich, Nucl. Phys. **B422** [FS] (1994) 541.
29. T. Morris, Phys. Lett. **B329** (1994) 241.
30. M.M. Tsypin, Phys. Rev. Lett. **73** (1994) 2015; preprint FIAN/TD–23/95 (hep-lat/9601021).
31. B. Bergerhoff, F. Freire, D. Litim, S. Lola, C. Wetterich, Phys. Rev. **B53** (1996) 5734; B. Bergerhoff, D. Litim, S. Lola and C.Wetterich, Int. J. Mod. Phys. **A11** (1996) 4273.
32. N. Tetradis and C. Wetterich, Nucl. Phys. **B398** (1993) 659.
33. U. Ellwanger and C. Wetterich, Nucl. Phys. **B423** (1994) 137.
34. D. J. Gross and F. A. Wilczek, Phys. Rev. Lett. **30** (1973) 1343; H. D. Politzer, Phys. Rev. Lett. **30** (1973) 1346.
35. See for instance M. Neubert, Phys. Rep. **245** (1994) 259.
36. J. Gasser and H. Leutwyler, Phys. Rep. **C87** (1982) 77; Nucl. Phys. **B250** (1985) 465; for a review see for instance H. Leutwyler, lectures given at the *Hadrons 96* workshop, Gramado, Brazil, 10 – 14 April 1994 (hep-ph/9406283).
37. G. 't Hooft, Phys. Rep. **142** (1986) 357.
38. J. L. Richardson, Phys. Lett. **82B** (1979), 272.
39. Y. Nambu and G. Jona–Lasinio, Phys. Rev. **122** (1961) 345.
40. J. Bijnens, Phys. Rep. **265** (1996) 369; T. Hatsuda and T. Kunihiro, Phys. Rep. **247** (1994) 221.
41. J. Pawlowski, preprint FSUJ-TPI-05-96 (hep-th/9605037).
42. D.–U. Jungnickel and C. Wetterich, preprint HD–THEP–96–19 to appear in Z. Phys. **C76** (1997) (hep-ph/9606483).
43. D.–U. Jungnickel and C. Wetterich, Phys. Lett. **389B** (1996) 600 (hep-ph/9607411).
44. D.–U. Jungnickel and C. Wetterich, preprint HD–THEP–97–9 to appear in Z. Phys. **C77** (1997) (hep-ph/9704345).
45. K.–I. Aoki, K. Morikawa, J.–I. Sumi, H. Terao and M. Tomoyose, Progr. Theor. Phys. **97** (1997) 479 (hep-ph/9612459).
46. W.A. Bardeen, C.T. Hill and D.–U. Jungnickel, Phys. Rev. **D49** (1994) 1437.

47. D.–U. Jungnickel and C. Wetterich, Phys. Rev. **D53** (1996) 5142.
48. C.G. Callan, Phys. Rev. **D2** (1970) 1541; K. Symanzik, Comm. Math. Phys. **18** (1970) 227.
49. S. Coleman and E. Weinberg, Phys. Rev. **D7** (1973) 1888.
50. M. Gell–Mann and M. Levy, Nuovo Cim. **16** (1960) 705.
51. M. Jamin and M. Münz, Z. Phys. **66** (1995) 633; K.G. Chetyrkin, C.A. Dominguez, D. Pirjol and K. Schilcher Phys. Rev. **D51** (1995) 5090; J. Bijnens, J. Prades and E. de Rafael, Phys. Lett. **B348** (1995) 226.
52. J. Berges, D.–U. Jungnickel and C. Wetterich, preprint HD–THEP–97–20 (hep-ph/9705474).
53. J. Adams, J. Berges, S. Bornholdt, F. Freire, N. Tetradis and C. Wetterich, Mod. Phys. Lett. **A10** (1995) 2367 (hep-th/9507093).
54. J. Berges and C. Wetterich, Nucl. Phys. **B487** (1997) 675 (hep-th/9609019).
55. H. Leutwyler, preprint HEPPH–9609467 (hep-ph/9609467).
56. For a recent review see H. Meyer–Ortmanns, Rev. Mod. Phys. **68** (1996) 473 (hep-lat/9608098).
57. Proceedings of Quark Matter '96, Nucl. Phys. **A610** (1996).
58. R.D. Pisarski and F. Wilczek, Phys. Rev. **D29** (1984) 338.
59. K. Rajagopal and F. Wilczek, Nucl. Phys. **B399** (1993) 395. Nucl. Phys. **B399** (1993) 577.
60. K. Rajagopal, in *Quark-Gluon Plasma 2*, edited by R. Hwa, World Scientific (1995) (hep-ph/9504310).
61. A. A. Anselm, Phys. Lett. **217B** (1988) 169; A. A. Anselm and M. G. Ryskin, Phys. Lett. **266B** (1991) 482; J.–P. Blaizot and A. Krzywicki, Phys. Rev. **D46** (1992) 246; J. D. Bjorken, Int. J. Mod. Phys. **A7** (1992) 4189; Acta Phys. Pol. **B23** (1992) 561; K. L. Kowalski and C. C. Taylor, preprint CWRUTH-92-6 (1992) (hep-ph/9211282); J. D. Bjorken, K. L. Kowalski and C. C. Taylor, in Proceedings of Les Rencontres de Physique de la Vallée D'Aoste, La Thuile, SLAC-PUB-6109 (1993); and in Proceedings of the workshop on Physics at Current Accelerators and the Supercollider, Argonne (1993) hep-ph/9309235.
62. C.M.G. Lattes, Y. Fujimoto and S. Hasegawa, Phys. Rep. **65** (1980) 151.
63. E. Shuryak, Comm. Nucl. Part. Phys. **21** (1994) 235.
64. See for instance J. Kapusta, *Finite Temperature Field Theory*, Cambridge University Press (1989).
65. P. Ginsparg, Nucl. Phys. **B170** (1980) 388; T. Appelquist and R. Pisarski, Phys. Rev. **D23** (1981) 2305; S. Nadkarni, Phys. Rev. **D27** (1983) 917; N.P. Landsman, Nucl. Phys. **B322** (1989) 498.
66. B. Widom, J. Chem. Phys. **43** (1965) 3898.
67. D. Toussaint, Phys. Rev. **D55** (1997) 362 (hep-lat/9607084).
68. E. Brezin, D.J. Wallace and K.G. Wilson, Phys. Rev. **B7** (1973) 232.
69. K. Kanaya and S. Kaya, Phys. Rev. **D51** (1995) 2404.
70. G. Baker, D. Meiron and B. Nickel, Phys. Rev. **B17** (1978) 1365.
71. J. Zinn–Justin, *Quantum Field Theory and Critical Phenomena* (Oxford University Press, 1993).
72. T.R. Morris and M.D. Turner, preprint SHEP–97–06 (hep-th/9704202).
73. P. Butera and M. Comi, Phys. Rev. **B52** (1995) 6185.
74. T. Reisz, Phys. Lett. **360B** (1995) 77 (hep-lat/9507011).
75. C. Bernard et al., Phys. Rev. **D55** (1997) 6861 (hep-lat/9612025); C. Bernard et al., Nucl. Phys. Proc. Suppl. **53** (1997) 442 (hep-lat/9608026).
76. S. Gottlieb et al., Phys. Rev. **D55** (1997) 6852 (hep-lat/9612020).
77. F. Karsch, Phys. Rev. **D49** (1994) 3791; F. Karsch and E. Laermann, Phys. Rev. **D50** (1994) 6954.
78. Y. Iwasaki, K. Kanaya, S. Kaya and T. Yoshie, Phys. Rev. Lett. **78** (1997) 179 (hep-lat/9609022).
79. G. Boyd, F. Karsch, E. Laermann and M. Oevers, Talk given at 10th International Conference on Problems of Quantum Field Theory, Alushta, Ukraine, 13-17 May 1996 (hep-lat/9607046).
80. A. Ukawa, Nucl. Phys. Proc. Suppl. **53** (1997) 106 (hep-ph9612011); S. Aoki, T. Kaneda, A. Ukawa and T. Umemura, Nucl. Phys. Proc. Suppl. **53** (1997) 438 (hep-lat/9612010).
81. J. Gasser and H. Leutwyler, Phys. Lett. **184B** (1987) 83; H. Leutwyler, Nucl. Phys. Proc. Suppl. **B4** (1988) 248.
82. C. Bernard et al., Phys. Rev. Lett. **78** (1997) 598 (hep-lat/9611031).
83. J.B. Kogut, J.F. Lagae and D.K. Sinclair, Nucl. Phys. Proc. Suppl. **53** (1997) 269 (hep-lat/9608128).